CD177, a specific marker of neutrophil activation, is associated with coronavirus disease 2019 severity and death

Yves Lévy, Aurélie Wiedemann, Boris P. Hejblum, Mélany Durand, Cécile Lefebvre, Mathieu Surénaud, Christine Lacabaratz, Matthieu Perreau, Emile Foucat, Marie Déchenaud, et al.

CD177, a specific marker of neutrophil activation, is associated with COVID-19 severity and death

Yves Lévy[1,2*$], Aurélie Wiedemann[1¥], Boris P. Hejblum [1,3¥], Mélany Durand [1,3], Cécile Lefebvre[1], Mathieu Surénaud[1], Christine Lacabaratz[1], Matthieu Perreau[4], Emile Foucat[1], Marie Déchenaud[1], Pascaline Tisserand[1], Fabiola Blengio[1], Benjamin Hivert[3], Marine Gauthier[3], Minerva Cervantes-Gonzalez[5,6,7], Delphine Bachelet[5,7], Cédric Laouénan[5,7], Lila Bouadma[8], Jean-François Timsit[8], Yazdan Yazdanpanah[6,7], Giuseppe Pantaleo[1,4,9], Hakim Hocini[1†], Rodolphe Thiébaut [1,3,10* †] and the French COVID cohort study group[a]

Affiliations

1. Vaccine Research Institute, Université Paris-Est Créteil, Faculté de Médecine, INSERM U955, Team 16, Créteil, France.
2. Assistance Publique-Hôpitaux de Paris, Groupe Henri-Mondor Albert-Chenevier, Service Immunologie Clinique, Créteil, France
3. Univ. Bordeaux, Department of Public Health, Inserm Bordeaux Population Health Research Centre, Inria SISTM, UMR 1219; Bordeaux, France
4. Swiss Vaccine Research Institute, Lausanne University Hospital, University of Lausanne, Lausanne, Switzerland
5. AP-HP, Hôpital Bichat, Département Épidémiologie Biostatistiques et Recherche Clinique, INSERM, Centre d'Investigation clinique-Epidémiologie Clinique 1425 F-75018 Paris, France
6. AP-HP, Hôpital Bichat, Service de Maladies Infectieuses et Tropicales, F-75018 Paris, France
7. Université de Paris, INSERM, IAME UMR 1137, F-75018 Paris, France
8. APHP- Hôpital Bichat – Médecine Intensive et Réanimation des Maladies Infectieuses, Paris, France
9. Immunology and Allergy Service, Department of Medicine; Lausanne University Hospital, University of Lausanne, Lausanne, Switzerland.

10. CHU de Bordeaux, Pôle de Santé Publique, Service d'Information Médicale, Bordeaux, France

[$] Lead contact

***Correspondence:** Pr. Yves Lévy, Vaccine Research Institute, INSERM U955, Hopital Henri Mondor, 51 Av Marechal de Lattre de Tassigny, 94010 Créteil, France, Phone: +33 (0) 1 49 81 44 42, Fax: +33 (0) 1 49 81 24 69, E-mail: yves.levy@aphp.fr & Pr Rodolphe Thiébaut, Université de Bordeaux, INSERM U1219 Bordeaux Population Health, 146 Rue Leo Saignat 33076 Bordeaux Cedex, France, Phone : +33 (0) 5 57 57 45 21, Fax : +33 (0) 5 56 24 00 81, E-mail: rodolphe.thiebaut@u-bordeaux.fr

[¥]these authors contributed equally to this work

[†] Senior authors

[a] Members of the French COVID study group are in listed in Supplementary Information

Abstract

The identification of COVID-19 patients with high-risk of severe disease is a challenge in routine care. We performed cell phenotypic, serum and RNA-seq gene expression analyses in severe hospitalized patients (n = 61). Relative to healthy donors, results showed abnormalities of 27 cell populations and an elevation of 42 cytokines, neutrophil chemo-attractants, and inflammatory components in patients. Supervised and unsupervised analyses revealed a high abundance of *CD177*, a specific neutrophil activation marker, contributing to the clustering of severe patients. Gene abundance correlated with high serum levels of CD177 in severe patients. Higher levels were confirmed in a second cohort and in ICU than non-ICU patients (P< 0.001). Longitudinal measurements discriminated between patients with the worst prognosis, leading to death, and those who recovered (P = 0.01). These results highlight neutrophil activation as a hallmark of severe disease and CD177 assessment as a reliable prognostic marker for routine care.

Introduction

The Coronavirus Disease 2019 (COVID-19) pandemic is caused by a newly described highly pathogenic beta coronavirus, Severe Acute Respiratory Syndrome coronavirus 2 (SARS-CoV-2) (Coronaviridae Study Group of the International Committee on Taxonomy of, 2020; Phelan et al., 2020). COVID-19 consists of a spectrum of clinical symptoms that range from mild upper respiratory tract disease in most cases to severe disease that affects approximately 15% of patients requiring hospitalization (Wu and McGoogan, 2020), some of whom require intensive care because of severe lower respiratory tract illness, acute respiratory distress syndrome (ARDS), and extra-pulmonary manifestations, leading to multi-organ failure and death. Several recent studies have provided important clues about the physiopathology of COVID-19 (Blanco-Melo et al., 2020; Chen et al., 2020a; Kuri-Cervantes et al., 2020; Mehta et al., 2020; Qin et al., 2020). Most compared the immune and inflammatory status of patients at different stages of the disease (Hadjadj et al., 2020; Mathew et al., 2020; Wilk et al., 2020). Thus, several important biomarkers associated with specific phases of the evolution of COVID-19 have thus far been identified (Ponti et al., 2020; Silvin et al., 2020). Inflammation, cytokine storms, and other dysregulated immune responses have been shown to be associated with severe disease pathogenesis (Lucas et al., 2020; Ong et al., 2020). Severe COVID-19 patients are characterized by elevated numbers of monocytes and neutrophils and lymphopenia (Giamarellos-Bourboulis et al., 2020; Huang et al., 2020; Mathew et al., 2020; Zhou et al., 2020), and a high neutrophil to lymphocyte ratio predicts in-hospital mortality of critically-ill patients (Fu et al., 2020). High levels of pro-inflammatory cytokines, including IL-6,IL-1β, TNF, MCP-1, IP-10, and G-CSF, in the plasma (Chen et al., 2020a; Chen et al., 2020b; Giamarellos-Bourboulis et al., 2020; Mathew et al., 2020; Zhou et al., 2020) and a possible defect in type I interferon activity have been reported in patients with severe COVID-19 (Arunachalam et al., 2020; Hadjadj et al., 2020; Ong et al., 2020). However, these responses are dynamic, changing rapidly during the clinical course of the disease, which may explain the high variability of the immunological

spectrum described (Arunachalam et al., 2020; Bouadma et al., 2020; Lucas et al., 2020). This makes it difficult to deduce a unique profile of the pathophysiology of this infection, which is still undetermined. Furthermore, the high amplitude of the signals generated by the inflammation associated with the disease may hide other pathways that are involved.

From a clinical standpoint, clinicians face the daily challenge of predicting worsening patients due to the peculiar clinical course of severe COVID-19, characterized by a sudden deterioration of the clinical condition 7 to 8 days after the onset of symptoms. Determination of the onset of the pathological process once infection has been established in a patient with a severe stage of infection is highly imprecise because of the possible pauci- or asymptomatic phase of the infection, as well as the low specificity of self-limited “flu” illness.

We used a systems immunology approach to identify host factors that were significantly associated with the time to illness onset, severity of the disease (ICU or transfer to ICU), and mortality of COVID-19 patients enrolled in the multicentric French COVID cohort (Yazdanpanah, 2020). In addition to the depletion of T cells and mobilization of B cells, neutrophil activation, and severe inflammation, we show upregulation of *CD177* gene expression and protein levels in the blood of COVID-19 patients in both the COVID-19 cohort and a “confirmatory” cohort, i.e., Swiss cohort, relative to healthy subjects. CD177, a neutrophil activation marker, characterized critically ill patients and marked disease progression and death. Our finding highlights the major role of neutrophil activation through CD177 over-expression in the critical clinical transition point in the trajectory of COVID-19 patients.

Results

Overview of the phenotype, cytokine, and inflammatory profiles of COVID-19 patients

Patient characteristics from the French COVID cohort enrolled in this analysis are shown in Table 1. All patients from this cohort were stratified as severe according to criteria of the French COVID cohort (clinicaltrials.gov NCT04262921) (Yazdanpanah, 2020), with 53 (87%) hospitalized in an ICU (either initially or after clinical worsening or death) and eight not. The median age was 60 years ([interquartile range (IQR)], [50-69]) and 80% were male. Sampling for immunological analyses was performed within three days of entry and after a median of 11 days [7-14] after symptoms onset. We first assessed leukocyte profiles by flow cytometry using frozen peripheral blood mononuclear cells (PBMCs) from 50 COVID-19 patients (with available PBMC samples) and 18 healthy donors (HDs) (14 or 15 HDs were used as controls per immune-cell subset).

We analyzed 52 immune cell populations (gating strategies are shown in Figure S1), of which 23 showed significant differences (Wilcoxon test adjusted for multiple comparisons) between the COVID-19 patients and HDs. We not only confirmed previously reported abnormalities but also revealed new immunological features of COVID-19 patients (Figure S2). The COVID-19 patients showed a significant reduction in the frequency of total $CD3^+$ T cells and $CD8^+$ T cells relative to HDs, as previously reported (De Biasi et al., 2020; Xu et al., 2020), that expressed an activated phenotype ($CD38^+HLA\text{-}DR^+$) (Figure 1A). The COVID-19 patients also showed lower frequencies of resting memory B cells contrasting with higher frequencies of activated memory B cells and exhausted B cells (Figure 1B). As previously reported (Bouadma et al., 2020; Mathew et al., 2020), the proportion of plasmablasts was markedly higher in COVID-19 patients (median [Q1-Q3]: 10.85% [3-23]) than HDs (0.76% [0.4-0.8]) ($P < 0.001$). Total NK-cell frequencies, more precisely those of the $CD56^{bright}$ and $CD56^{dim}CD57^-$ NK-cell subpopulations, were lower than in HDs ($P = 0.017$, $P < 0.001$, and $P = 0.004$, respectively) (Figure 1C), while a higher proportion of these NK cells, as well as NKT cells, were cycling, expressing Ki67 antigen ($CD56^{bright}$: 22% [13-30], $CD56^{dim}CD57^-$:

16.8% [11.5-27], and NKT: 10% [5.6-18.2]) (P = 0.003, P = 0.004, and P = 0.001 compared to HD) (Figure 1C). In addition, COVID 19-patients showed significantly smaller classical ($CD14^+CD16^-$), intermediate ($CD14^+CD16^+$), and non-classical ($CD14^-CD16^+$) monocyte subpopulations than HDs (P = 0.013, P = 0.017, P < 0.001, respectively) (Figure 1D). Interestingly, COVID-19 patients tended to exhibit a higher frequency of γδ T cells than HDs (median 10.4% [7.5-16.1] vs 7.3% [6-10] in HDs; P = 0.068) (Figure 1E), with a significant proportion of γδ T cells showing higher expression of the activation marker CD16 (P = 0.01) and lower expression of the inhibitory receptor NKG2A (P < 0.001) than HDs (Figure 1E). Finally, we observed markedly smaller frequencies of dendritic cells (DCs) for all populations studied (pre-DC, plasmacytoid DC (pDC), and conventional DC (cDC1 and cDC2) in COVID-19 patients than in HDs (P < 0.001, for all comparisons) (Figure 1F). Neutrophils count were available in 44 patients and the concentration was more elevated in COVID19 patients belonging to group 2 and group 3 compared to group 1 (8.109/L vs 3.109/L, p<0.03). It was also more elevated in patients hospitalized in ICU (8.109/L vs 2.109/L, p<0.009).

We then evaluated the levels of 71 serum cytokines, chemokines, and inflammatory factors in 33 COVID-19 patients and 5 HDs. Forty-four analytes differed significantly (Wilcoxon test adjusted for multiple comparisons) between the COVID-19 patients and HDs (shown in the heatmap in Figure 2 and detailed in Figure S3). The levels of 42 factors were higher, among them, pro-inflammatory factors (IL-1a, IL-6, IL-18, tumor necrosis factor-α and β (TNF-α, TNF-β), IL-1ra, ST2/IL-1R4, the acute phase protein lipopolysaccharide binding protein LBP, IFN-a2); Th1 pathway factors (IL-12 (p70), IFN-γ, IP-10, IL-2Ra); Th2/regulatory cytokines (IL-4, IL-10, IL-13); IL-17, which also promotes granulocyte-colony stimulating factor (G-CSF)-mediated granulopoiesis and recruits neutrophils to inflammatory sites; T-cell proliferation and activation factors (IL-7, IL-15); growth factors (SCF, SCGF-b, HGF, b-FGF, b-NGF); and a significant number of cytokines and chemokines involved in macrophage and neutrophil activation and chemotaxis (RANTES (CCL5), MIP-1a and b (CCL3 and CCL4), MCP-1 (CCL2), MCP-3 (CCL7), M-CSF, MIF, Gro-a (CXCL1), monokine inducible by γ

interferon MIG/CXCL9, IL-8, IL-9). Interestingly, we found higher levels of midkine, a marker usually not detectable in the serum, which enhances the recruitment and migration of inflammatory cells and contributes to tissue damage (Cai et al., 2020). In parallel, Granzyme B and IL-21 levels were significantly lower in COVID-19 patients than HDs ($P = 0.007$ and $P = 0.004$, respectively) (Figure S3).

Whole blood gene expression profiles show a specific signature for COVID-19 patients

The comparison of gene abundance in whole blood between COVID-19 patients (n = 44) and HDs (n = 10) showed 4,079 differentially expressed genes (DEG) with an absolute fold change ≥ 1.5, including 1,904 that were upregulated and 2,175 that were downregulated (Figure 3A). The main pathways associated with the DEG correspond to the immune response, including neutrophil and interferon signaling, T and B cell receptor responses, metabolism, protein synthesis, and regulators of the eIF2 and mammalian target of rapamycin (mTOR) signaling pathways (Figure 3A). Although several of these pathways involved multiple cell types, analysis of the neutrophil pathway showed higher abundance of genes mainly related to neutrophil activation, their interaction with endothelial cells, and migration (Figure 3B). Among the most highly expressed genes, this signature included *CD177*, a specific marker of neutrophil adhesion to the endothelium and transmigration (Bayat et al., 2010), *HP* (Haptoglobin), a marker of granulocyte differentiation and released by neutrophils in response to activation (Theilgaard-Monch, 2006), *VNN1* (hematopoietic cell trafficking), *GPR84* (neutrophil chemotaxis), *MMP9* (neutrophil activation and migration), and *S100A8* and *S100A12* (neutrophil recruitment, chemotaxis, and migration). The *S100A12* protein is produced predominantly by neutrophils and is involved in inflammation and the upregulation of vascular endothelial cell adhesion molecules (Roth et al., 2003) (Figure 3B).

In parallel, we observed a higher abundance of several interferon stimulating genes (ISG) (*IFI27*, *IFITM3*, *IFITM1*, *IFITM2*, *IFI6*, *IRF7*, *IRF4*) (Figure 3C) and cytokines and cytokine receptors *(IL-1R*, *IL-18R1*, *IL-18RAP*, *IL-4R*, *IL-17R*, *IL-10*) (Figure 3D). Consistent with profound T-cell lymphopenia, the expression of several families of T-cell Receptor (TCRA)

genes was lower (Figure 3E). We observed severe dysregulation of T-cell function that involved inhibition of serine/threonine kinase PKCθ signaling (z-score = -4.46), as well as the inducible T-cell co-stimulator/ICOSL axis (z-score = -4.5) (Figure S4). In contrast to the results for T cells, the peripheral expansion of memory B cells and plasmablasts was associated with broad expansion of the B-Cell Receptor (BCR) (Figure 3F and Table S2).

We also observed genes belonging to several crucial pathways and biological processes that had not been previously reported to characterize COVID-19 patients to be underrepresented. These included eIF2 signaling, with many downregulated genes, such as ribosomal proteins (RP) and eukaryotic translation initiation factors (EIFs) (Figure S4A), common targets of the integrated stress response (ISR), including antiviral defense (Levin and London, 1978; Pakos-Zebrucka et al., 2016). In addition, we also found genes involved in signaling through mTOR (Figure S4B), a member of the phosphatidylinositol 3-kinase-related kinase family of protein kinases. Prediction analysis using Ingenuity pathways showed both lower eIF2 (z-score = - 6.8) and mTOR (z-score = -2.2) signaling in COVID-19 patients than HDs.

Unsupervised whole blood gene expression profiles reveal distinct features of COVID-19 patients.

Unsupervised classification of 44 COVID-19 patients and 10 HDs identified three distinct groups of COVID-19 patients: 10 in group 1, 16 in group 2, and 18 in group 3 (Figure 4). Detailed patient characteristics according to group are presented in Table S1. Among a large set of clinical and biological characteristics, the analysis showed the differential clustering to not be explained by the severity of the disease. Indeed, the median Sequential Organ Failure Assessment (SOFA) score and Simplified Acute Physiology Score (SAPS2), which include a large number of physiological variables (Le Gall, 1993; Vincent et al., 1998) and evaluate the clinical severity of the disease (a high score is associated with a worse prognosis) of the COVID-19 patients, were 6 [4-7] and 36 [28-53], respectively, with no significant differences between groups. Nevertheless, we observed a significant difference from symptoms onset to the admission, which ranged from 7 [6 –11] days for patients in group 1 to 11 [10-14] and 13

[9-14] days for patients in groups 2 and 3, respectively (P = 0.04, Kruskal-Wallis test). Finally, group 1 which was the closest to HDs in terms of gene profile, consisted of patients in the early days of the disease (Table S1).

Analysis of the genes contributing to the differences between groups confirmed and extended the findings described above (Figure 3 and Figure S4). Several pathways were highly represented in sectors of the heatmap defined according to gene abundance across patient groups. For example, 97% of the genes making up the BCR and 65% of those involved in neutrophil responses were represented among the genes showing a greater abundance in COVID-19 groups 2 and 3 than group 1 and HDs (Figure 4). Other pathways, such as those for interferon (64%), TCR (100%), iCOS-iCOS-L (88%), mTOR (81%), and eIF2 signaling (92%) were also highly represented. The interferon signaling genes, such as *IFI44L*, *IFIT2*, and *IRF8*, a regulator of type I Interferon (α, β), were significantly more abundant at earlier stages (in patients from group 2) and tended to be less abundant in group 3, at more advanced stages of the disease. Finally, the abundance of genes belonging to T-cell pathways (TCR, iCOS-iCOSL signaling) or mTOR and eIF2 signaling was lower in group 3, that is to say, those who were analyzed after a longer time from symptom onset to the admission. The findings described above highlight the heterogeneity of COVID-19 patients.

Integrative analysis of all biomarkers reveals the major contribution of CD177 in the clinical outcome of COVID-19 patients.

We performed an integrative analysis using all available data to disentangle the relative contribution of the various markers at the scale of every patient. We thus pooled the data for 29,302 genes from whole blood RNA-seq, cell phenotypes (52 types), and cytokines (71 analytes) using the recently described MOFA approach (Argelaguet et al., 2019), which is a statistical framework for dimension reduction adapted to the multi-omics context. The data are reduced to components that are linear combinations of variables explaining inter-patient variability across the three biological measurement modalities. The first component, that we called our integrative score, discriminated between the three groups of COVID-19 patients

241 (initially defined by hierarchical classification based on gene abundance only) and HDs
242 (Figure 5A), although it only explained a portion of the variability within each of the three
243 types of markers (14% of gene expression, 14% of cell phenotypes, and 5% of cytokines).
244 Figures 5 B-D showed the contribution of each type of markers to the integrative score. The
245 main contributors for the cell phenotype were the significantly lower frequency of cDC2 and T
246 cells and, marginally, the higher number of plasmablasts and $CD16^{+}$ γδ T cells in COVID-19
247 patients (Figure 5B). The contribution of soluble factors was marked by higher levels of
248 soluble CD163 (sCD163), a marker of polarized M2 macrophages involved in tissue repair
249 (Zhi et al., 2017), in more advanced COVID-19 groups (Figure 5C). Indeed, CD163 gene
250 expression was also significantly higher in COVID-19 patients than HDs (log2 fold change =
251 +1.55; FDR = $4.79\ 10^{-2}$). sCD163 has also been reported to be a marker of disease severity
252 in critically ill patients with various inflammatory or infectious conditions (Buechler et al.,
253 2013). Interestingly, the genes that contribute the most to the synthesis of this factor were
254 part of the neutrophil module (*CD177*, *ARG1*, *MMP9*) (Figure 5D). Integrated analysis also
255 revealed higher expression of proprotein convertase subtilisin/kexin type 9 (*PCSK9*). High
256 plasma PCSK9 protein levels highly correlate with the development and aggravation of
257 subsequent multiple organ failure during sepsis (Boyd et al., 2016; Dwivedi et al., 2016). Of
258 note, high PCSK9 levels have been recently associated with severe Dengue infection (Gan
259 et al., 2020). Finally, the increasing abundance of CD177 gene expression according to
260 group was again clearly apparent (Figure S4). An additional cell-type specific significance
261 analysis (csSAM) has been performed to check the robustness of the CD177 differential
262 expression according to the cell-type frequencies (Shen-Orr et al., 2010). We found that
263 CD177 differential expression between COVID-19 and HD patients was not fully explained by
264 population variations. Indeed, it remained significant after deconvolution in several
265 leucocytes subpopulations (notably FDR of 0.04 within T-cells and 0.03 within Monocytes).
266

Serum CD177 protein levels are associated with the clinical outcome of COVID-19 patients.

Given the contribution of the neutrophil activation pathway in the clustering of COVID-19 patients, we sought neutrophil-activation features that could act as possible reliable markers of disease evolution. We focused on CD177 because: i) it is a neutrophil-specific marker representative of neutrophil activation, ii) it was the most highly differentially expressed gene in patients, and iii) the protein can be measured in the serum, making its use as a marker clinically applicable. Thus, we used an ELISA to quantify CD177 in the serum of 203 COVID-19 patients (115 patients from the French cohort and 88 patients from the Swiss COVID-19 cohort that we used as "a confirmatory" cohort, patient characteristics are described in Table 2), 21% of whom the measurements were repeated (from 2 to 10 measurements per individual). First, we confirmed the significantly higher median serum protein level in the global cohort of COVID-19 patients (4.5; [2.2-7.4]) relative to that of 16 HDs (2.2 [0.9-4.2]) ($P = 0.015$, Wilcoxon test) (Figure 6A). Second, we found a robust agreement between CD177 gene expression measured by RNA-seq and CD177 protein levels measured by ELISA (intraclass correlation coefficient 0.88), (Figure 6B).

Then, we examined the association of clinical characteristics and outcomes with serum CD177 concentration at the time of admission. The serum CD177 concentration was positively associated with the time from symptom onset to the admission ($r=0.22$, $P = 0.0026$) (Figure 6C) and was higher for patients hospitalized in an ICU (6.0 ng/ml [3.5-9.4] vs 3.3 ng/ml [1.5-5.6], $P < 0.001$) (Figure 6D). The association between serum CD177 levels and hospitalization in an ICU was independent of the usual risk factors, such as age, sex, chronic cardiac or pulmonary diseases, or diabetes (multivariable logistic regression, adjusted odds ratio 1.14 per unit increase, $P < 0.001$). We observed a trend towards a positive association with the SOFA and SAPS2 risk scores that was not statistically significant ($P = 0.17$ and $P = 0.074$, respectively) (Figure S6A and B). CD177 levels were not associated with other conditions that contribute to a high risk of severe disease, such as diabetes ($P = 0.632$),

chronic cardiac disease (P = 0.833), chronic pulmonary disease (P = 0.478), or age of the patient (P = 0.83).

We then examined the dynamics of the CD177 concentration in 172 COVID-19 patients, with longitudinal serum samples, using all available measurements (Figure 6E). At the first measurement, the average concentration of CD177 was not significantly different between the patients who died and those who recovered (5.93 vs 5.06, P= 0.26, Wald test). When looking at the change of CD177 concentration over time, it appears clearly that the concentration was decreasing in those who recovered (-0.22 ng/mL/day, 95% CI -0.307; -0.139) whereas it was stable in those who died later on (+0.10 ng/mL/day, 95% CI -0.014; +0.192). These results show that the stability of CD177 protein levels in severe COVID-19 patients during the course of the disease is a hallmark of a worse prognosis, leading to death.

Discussion

Here, we investigated factors that influence the clinical outcomes of severe COVID-19 patients involved in a multicentric French cohort combining standardized whole-blood RNA-Seq analyses, in-depth phenotypic analysis of immune cells, and measurements of a large panel of serum analytes. An integrated and global overview of host markers revealed several pathways associated with the course of COVID-19 disease, with a prominent role for neutrophil activation. This signature included CD177, a specific neutrophil marker of activation, adhesion to the endothelium, and transmigration. The correlation between *CD177* gene abundance and serum protein levels in the blood of COVID-19 patients underscores the importance of this marker, making the measurement of CD177 protein levels a reliable approach that is largely accessible in routine care. We also demonstrated that the dynamics of serum CD177 levels is strongly associated with the severity of COVID-19 disease, ICU hospitalization, and survival in an additional cohort of patients. During follow-up, the CD177 protein levels decrease in patients who are recovering while staying high in those who died

CD177 is a glycosylphosphatidylinositol (GPI)-anchored protein expressed by a variable proportion of human neutrophils. It plays a key role in the regulation of neutrophils by modulating their migration and activation. For example, the CD177 molecule has been identified as the most dysregulated parameter in purified neutrophils from septic shock patients (Demaret et al., 2016) and in severe influenza (Tang et al., 2019). Clinically, neutrophil chemotaxis, infiltration of endothelial cells, and extravasation into alveolar spaces have been described in lung autopsies from deceased COVID-19 patients (Fu et al., 2020). Elevated *CD177* mRNA expression has also been described for patients with acute Kawasaki Disease (KD) (Huang et al., 2019) and resistant to IV Ig therapy (Jing et al., 2020; Ko et al., 2019), a syndrome that has been described as a possible complication of SARS-CoV-2 infection in children (Toubiana et al., 2020; Viner and Whittaker, 2020). Our results are also consistent with those obtained using animal models, suggesting an important role for neutrophil activation in the severity of infection with respiratory viruses through their

migration towards infected lungs, and in humans infected with influenza (Brandes et al., 2013; Narasaraju et al., 2011; Zaas et al., 2009) .

The neutrophil activation signature is a specific feature of the homing of activated neutrophils toward infected lung tissue in acute lung injury (Juss et al., 2016), followed by the initiation of aggressive responses and the release of neutrophil extracellular traps (NETs), leading to an oxidative burst and the initiation of thrombus formation (Darbousset et al., 2012). Previous studies have reported elevated levels of circulating NETs in COVID-19 disease (Barnes et al., 2020a). Consistent with this finding and extending these data, we showed the differential expression of NET-related genes (Brandes et al., 2013; Narasaraju et al., 2011; Tang et al., 2019) (*S100A8*, *S100A9*, and *S100A12*), confirming the recently described elevated expression of calprotectin (heterodimer of S100A8 and A9) in severe COVID-19 patients (Silvin et al., 2020). The association of neutrophil activation signature with COVID-19 severity has also been described recently with *CD177* gene being one of the most differentially expressed gene in advanced disease (Aschenbrenner et al., 2021; Schulte-Schrepping et al., 2020). Likely, we believe that our data extended significantly these recent observations showing that CD177 is increased both at the level of coding RNA and at the protein level. Moreover, we show also that CD177 is not only a marker of severity but also of death as revealed by the longitudinal analysis which was confirmed in a second cohort.

Although, it is difficult to formally conclude whether CD177 is a causal factor of disease progression or a consequence of the severity of the disease, our data strongly show that CD177 is a valid hallmark of the physiopathology of COVID-19. This observation suggests that the activation of neutrophils, triggered by the infection, is a fundamental element of the innate response. However, persistent activation of this pathway may constitute, along with other factors (e.g., “cytokine storm”), fatal harm possibly associated with the critical turning point in the clinical trajectory of patients during the second week of the infection.

Neutrophil activation was associated with significant changes in the level of gene expression of several pathways, some concordantly associated with disturbances in immune-cell

populations and cytokine and inflammatory profiles. We reveal a complex picture of the activation of innate immunity, assessed by significant changes in the expression of several genes involved in interferon signaling and the response to stress and the production of inflammatory/activation markers, with a balance between pro-inflammatory signals (increased expression of IL-1R1, IL-18R1 and its accessory chain IL-18 RAP) and anti-inflammatory cytokines or regulators (increased expression of IL-10, IL-4R, IL-27, IL-1RN) (Kim et al., 2005; Migliorini et al., 2020). The frequency of γδ T cells, a subpopulation of $CD3^+$ T cells that were first described in the lung (Augustin et al., 1989) and that play critical roles in anti-viral immune responses, tissue healing, and epithelial cell maintenance (Cheng and Hu, 2017), was elevated and they expressed an activation marker (CD16) and low levels of the inhibitory receptor NKG2A, suggesting possible killing capacity. In accordance with our observation that eIF2 signaling is significantly inhibited in COVID-19 patients, recent studies have shown that coronaviruses encode ISR antagonists, which act as competitive inhibitors of eIF2 signaling (Rabouw et al., 2016; Rabouw et al., 2020). Similarly, the inhibition of mTOR signaling that we found in COVID-19 patients is consistent with the impaired mTOR signaling reported in blood myeloid dendritic cells of COVID-19 patients (Arunachalam et al., 2020). Interestingly, we observed a markedly smaller proportion of all DC (pre-DC, pDC, cDC1 and cDC2) and monocyte cell populations, including classical, intermediate, and non-classical subpopulations, in COVID-19 patients than in HDs. Based on these observations, it can be hypothesized that the impairment in IFN-α production observed in severe COVID-19 patients may be the result of both a decrease in the number of pDCs, which are natural IFN-producing cells (Ali et al., 2019), and inhibition of mTOR signaling, a regulator of IFN-α production, in these cells (Kaur et al., 2012).

We confirmed the previously reported expansion of B-cell populations (Arunachalam et al., 2020; Bouadma et al., 2020) in COVID-19 patients and our results showed that the anti-SARS-CoV-2 B cell repertoire is commonly mobilized. The marked upregulation of IGV gene families included the *IgHV1-24* family, described to be specific for COVID-19 (Brouwer et al.,

2020). The expanded *VH4-39* family was also recently reported to be the most highly represented in S-specific SARS-CoV-2 sequences (Brouwer et al., 2020). We also found enrichment of *VH3-33*, previously described in a set of clonally related anti-SARS-CoV-2 receptor-binding domain antibodies (Barnes et al., 2020b).

Globally, these results show that the defense against SARS-CoV-2 following pathogen recognition triggers a fine-tuned program that not only includes the production of antiviral (Interferon signaling) and pro-inflammatory cytokines but also signals the cessation of the response and a strong disturbance of adaptive immunity.

The same pathways (immune and stress responses through eIF2 signaling, neutrophil and Interferon signaling, T- and B-cell receptor responses, and mTOR pathways) contributed to the ability to discriminate between three groups of severe COVID-19 patients in an unsupervised analysis. One limitation of our study was that we did not repeat the RNA-seq analyses in these specific groups of patients. Nonetheless, it is noteworthy that these groups differed significantly by the time from disease onset. These findings provide clues in our understanding of the wide range of profiles previously described for COVID-19 by showing that these patterns may be mainly related to time-dependent changes in the blood during the course of the infection (Laing et al., 2020; Ong et al., 2020). For example, the observed lower abundance of IFN signaling genes in the last group of COVID-19 patients may be due to decreased abundance in more advanced disease and/or patients who constitutively present a lower abundance of ISG, as described in previous studies (Bastard et al., 2020).

Several months after the emergence of this new disease, treatment options for patients with severe disease requiring hospitalization are still limited to corticosteroids, which has emerged as the treatment of choice for critically ill patients (Prescott and Rice, 2020; Sterne et al., 2020). However, interventions that can be administered early during the course of infection to prevent disease progression and longer-term complications are urgently needed. A major obstacle for the design of “adapted “therapies to the various stages of disease evolution is a lack of markers associated with sudden worsening of the disease of patients with moderate

to severe disease and markers to predict improvement. Our results show that the measurement of CD177 during the course of the disease may be helpful in following the response to treatment and revision of the prognosis. In addition, they suggest that therapies aiming to control neutrophil activation and chemotaxis should be considered for the treatment of hospitalized patients.

Limitations of the study

Healthy donors were collected from the French Blood Donors Organisation (Etablissement Français du sang (EFS)) before the COVID-19 outbreak. Age to donate blood is limited between 18 and 65 years (with the necessary medical agreement beyond 60 years). Due to the age of hospitalized COVID-19 patients (median: 61 y.o), it was not possible to have age-matched HD. So we could not exclude that differences observed between HD and COVID-19 patients could be associated to the age difference. Samples were not available for the entire cohort of 61 patients for every experimentation but clinical characteristics were not different between included and excluded patients for each assay, that is cell phenotype (all $p > 0.97$), seric markers (all $p > 0.58$) and gene expression (all $p > 0.15$). Finally, although we have identified a set of gene characterizing activation of a neutrophil pathway in patients, as well as an association with increased serum CD177, a marker highly specific of neutrophils, we did not study the phenotype of blood neutrophils from patients included in our cohorts for practical reasons.

Acknowledgments

We thank the patients who donated their blood. We thank F. Mentre, S. Tubiana, the French COVID cohort, and REACTing (REsearch & ACtion emergING infectious diseases) for cohort management. We thank the scientific advisory board of the French COVID-19 cohort composed of Dominique Costagliola, Astrid Vabret, Hervé Raoul, and Laurence Weiss. We thank Romain Levy for fruitful discussions. This work was supported by INSERM and the Investissements d'Avenir program, Vaccine Research Institute (VRI), managed by the ANR under reference ANR-10-LABX-77-01. The French COVID Cohort is funded through the Ministry of Health and Social Affairs and Ministry of Higher Education and Research dedicated COVID19 fund and PHRC n°20-0424 and the REACTing consortium. Funding sources were not involved in the study design, data acquisition, data analysis, data interpretation, or writing of the manuscript.

Author Contributions

YL and AW conceived and designed the study. MC, JFT, YY, LB, DB, CLa, GP, and MP participated in sample and clinical data collection. EF, MDe, MS, CLe, and PT performed the experiments. MD, MG, BH, and CLe analyzed the data. YL, RT, AW, HH, MS, BJH, and CL analyzed and interpreted the data. YL, RT, AW, and HH drafted the first version and wrote the final version of the manuscript. All authors approved the final version.

Conflict of interest statement

None of the authors has any conflict of interest to declare.

Figure legends

Figure 1. **Frequency of immune-cell subsets between HD (n = 18) and COVID-19 patients (n = 50). A** Frequency of total CD3 T cells, CD4 and CD8 T-cell subsets, and activated $CD38^{+}HLADR^{+}$ CD8 T cells. **B** Frequency of B-cell subsets ($CD21^{+}CD27^{+}$: resting memory, $CD21^{-}CD27^{+}$: activated memory, $CD21^{-}CD27^{-}$: exhausted) and plasmablasts ($CD38^{++}CD27^{+}$) gated on $CD19^{+}$ B cells. **C** Frequency of NK-cell subsets (gated on $CD3^{-}CD14^{-}$) $CD56^{Bright}$: $CD56^{++}CD16^{+}$, $CD56^{dim}$: $CD56^{+}CD16^{++}CD57^{+/-}$, differentiated $Ki67^{+}$ NK cells (gated on $CD56^{Bright}$ or $CD56^{dim}CD57^{-}$ NK cells) and differentiated $Ki67^{+}$ NKT cells (gated on $CD3^{+}CD56^{+}$ cells). **D** Monocyte subsets (gated on $CD3^{-}CD56^{-}$) (classical monocytes: $CD14^{+}CD16^{-}$, intermediate monocytes: $CD16^{+}CD14^{+}$, non-classical monocytes: $CD14^{-}CD16^{+}$). **E** Frequency of γδ T cells (gated on $CD3^{+}$ T cells) and CD16 and NKG2A expression (gated on γδ CD3 T cells). **F** Frequency of DC subsets (gated on $HLADR^{+}Lin^{-}$) (pDC: $CD45RA^{+}CD33^{-}CD123^{+}$, pre-DC: $CD123^{+}CD45RA^{+}$, cDC1: $CD33^{+}CD123^{-}CD141^{+}CD1c^{low}$, cDC2: $CD33^{+}CD123^{-}CD14^{+}CD1c^{+}$) detected by flow cytometry in PBMCs from n = 50 COVID19 patients and n = 18 HDs. The differences between the two groups were evaluated using Wilcoxon rank sum statistical tests. The lower and upper boundaries of the box represent the 25% and 75% percentiles, the whiskers extend to the most extreme data point that is no more than 1.5 times the interquartile range away from the box. Median values (horizontal line in the boxplot) are shown. See also Figure S1 and S2

Figure 2. Heatmap of analyte abundance in serum. The colors represent standardized expression values centered around the mean, with variance equal to 1. HD: healthy donors (n = 5), COVID: COVID19 patients (n = 33). Each column represents a subject. Each line represents an analyte. See also Figure S3

Figure 3. Whole blood gene expression in COVID-19 patients and HDs. A. Volcano plot showing differentially expressed genes (DEG) according to the log2 fold change (log2 FC) and Benjamini-Hocberg False Discovery Rate (FDR) with thresholds at absolute log2 FC ≥ log2(1.5) and FDR ≤ 0.05. **B** Main top DEG related to neutrophils. **C** and **D** Main DEG related

to *IFN* and interleukin responses, respectively. **E** Main *TCRV* T-cell repertoire DEG **F** Main B-cell *IGHV* repertoire DEG. Red symbols represent overabundant genes in COVID-19 relative to HD, green symbols represent underabundant genes. See also Figure S4 and Table S2

Figure 4. Heatmap of standardized gene expression. The colors represent standardized expression values centered around 0, with variance equal to 1. Each column represents a subject. This heatmap was built by unsupervised hierarchical clustering of log2-counts-per-million RNA-seq transcriptomic data from whole blood (29,302 genes) and subjects (n = 54) using the Euclidean distance and Ward's method. Seven blocks are highlighted according to the features of gene expression across the groups of individuals. Enrichment (number and % of genes of a given pathway selected in the block) of pathways of interest are shown for each block. See also Table S1

Figure 5. Integrative analysis. Integrative analysis of the data of RNA-seq (29,302 genes) from 44 COVID-19 patients, cell phenotype (52 types) from 45 COVID-19 patients, and serum analytes (71 analytes) from 33 COVID-19 patients using a sparse principal component analysis approach, MOFA v2. **A** Integrative score according to the patient groups defined by the hierarchical clustering of the RNA-seq data. Top 10 marker contributions (according to the weight from -1 to 1) of the cell phenotypes (**B**), serum analytes (**C**), and RNA-seq (**D**). The integrative score corresponds to the first factor of the analysis and allows the ordering of individuals along an axis centered at 0. Individuals with an opposite sign for the factor therefore have opposite characteristics. See also Figure S5

Figure 6: Distribution of the CD177 marker and association with clinical outcomes of COVID-19 patients. A Measurement of CD177 (ng/ml). HD: Healthy donors (n = 16), COVID-19 patients (n = 203). The difference between the two groups was evaluated using Wilcoxon rank sum statistical tests. The median values (horizontal line in the boxplot) are shown. The lower and upper boundaries of the box represent the 25% and 75% percentiles. **B** Correlation between normalized *CD177* values of gene expression measured by RNA-seq

and CD177 protein by ELISA (ng/ml) from 36 COVID-19 patients. The blue line represents the linear regression line and the grey area the 95% prediction confidence interval. **C** Association between CD177 serum concentration and time from symptom onset to the admission (n = 192). This association was tested using Spearman correlation tests. The blue line represents the linear regression line and the grey area the 95% confidence interval. **D** Measurement of CD177 serum concentration in patients hospitalized in an intensive care unit (ICU) or not (n = 196). Wilcoxon rank tests were used. The median values (horizontal line in the boxplot) are shown. The lower and upper boundaries of the box represent the 25% and 75% percentiles. **E**. Change of CD177 concentration over time according to the occurrence of death for 172 COVID-19 patients and a total of 248 measurements. Predictions were calculated using a mixed effect models for longitudinal data. See also Figure S6

STAR Methods

Resource availability

Lead contact

Further information and requests for resources should be directed to and will be fulfilled by the lead contact, Yves Lévy (yves.levy@aphp.fr).

Materials availability

No materials were newly generated for this paper.

Data and code availability

RNA sequencing data that support the findings of this study have been deposited in Gene Expression Omnibus (GEO) repository with the accession codes GSE171110. Further information and requests for resources and reagents should be directed to and will be fulfilled by the Lead Contact: Yves Lévy (yves.levy@aphp.fr)

Experimental model and subject details

Subjects

We enrolled a subgroup of COVID19 patients of the prospective French COVID cohort in this immunological study which is part of the cohort main objectives. Median age of COVID19 patients was 60 years [50-69], 80% were male. Ethics approval was given on February 5th by the French Ethics Committee CPP-Ile-de-France VI (ID RCB: 2020-A00256-33). Eligible patients were those who were hospitalized with virologically confirmed COVID-19. Briefly, nasopharyngeal swabs were performed on the day of inclusion for SARS-CoV-2 testing according to WHO or French National Health Agency guidelines. Viral loads were quantified by real-time semi-quantitative reverse transcriptase polymerase chain reactions (RT-PCR) using either the Charité WHO protocol (testing the E gene and RdRp) or the Pasteur institute assay (testing the E gene and two other RdRp targets, IP2 and IP4). The study was conducted with the understanding and the consent of each participant or its surrogate covering the sampling, storage, and use of biological samples. The time from symptom onset to the admission has been retrospectively collected by the interview of patients enrolled in

549 the national “French Covid-19 cohort”. The Swiss cohort was approved by the ethical
550 commission (CER-VD; Swiss ethics protocol ID: 2020-00620) and all subjects provided
551 written informed consent. Blood from healthy donors was collected from the French Blood
552 Donors Organization (Etablissement Français du sang (EFS)) before the COVID-19
553 outbreak. HD characteristics are shown in Table S3.

554 **Method details**

555 ***Quantification of serum analytes***

556 In total, 71 analytes were quantified in heat-inactivated serum samples by multiplex magnetic
557 bead assays or ELISA. Serum samples from five healthy donors were also assayed as
558 controls. The following kits were used according to the manufacturers’ recommendations:
559 LXSAHM-2 kits for CD163,ST2,CD14 and LBP (R&D Systems); the LXSAHM-19 kit for IL-21,
560 IL-23, IL-31, EGF, Flt-3 Ligand, Granzyme B, Granzyme A, IL-25, PD-L1/B7-H1, TGF-α,
561 Aggrecan, 4-1BB/CD137, Fas, FasL,CCL-28, Chemerin, sCD40L, CXCL14, and Midkine
562 (R&D Systems); and the 48-Plex Bio-Plex Pro Human Cytokine screening kit for IL-1β, IL-
563 1rα, IL-2, IL-4, IL-5, IL-6, IL-7, IL-8 / CXCL8, IL-9, IL-10, IL-12 (p70), IL-13, IL-15, IL-17A /
564 CTLA8, Basic FGF (FGF-2), Eotaxin / CCL11, G-CSF, GM-CSF, IFN-γ, IP-10/CXCL10,
565 MCP-1 /CCL2, MIP-1α / CCL3, MIP-1β / CCL4, PDGF-BB (PDGF-AB/BB), RANTES/CCL5,
566 TNF-α, VEFG (VEGF-A), IL-1a, IL-2Ra (IL-2R), IL-3, IL-12 (p40), IL-16, IL-18, CTACK /
567 CCL27, GRO-a /CXCL1 (GRO), HGF, IFN-α2, LIF, MCP-3 / CCL7, M-CSF, MIF,
568 MIG/CXCL9, b-NGF, SCF, SCGF-b ,SDF-1α ,TNF-b/LTA, and TRAIL (Bio-Rad). The data
569 were acquired using a Bio-Plex 200 system. Extrapolated concentrations were used and the
570 out-of-range values were entered at the highest or lowest extrapolated concentration. Values
571 were standardized for each cytokine across all displayed samples (centered around the
572 observed mean, with variance equal to 1). CD177 quantification was performed on non-
573 inactivated serum samples (diluted 1:2 or 1:10) using a Human CD177 ELISA Kit
574 (ThermoFisher Scientific), according to the manufacturer’s instructions.

Cell phenotyping

Immune-cell phenotyping was performed using an LSR Fortessa 4-laser (488, 640, 561, and 405 nm) flow cytometer (BD Biosciences) and Diva software version 6.2. FlowJo software version 9.9.6 (Tree Star Inc.) was used for data analysis. CD4+ and CD8+ T cells were analyzed for CD45RA and CCR7 expression to identify the naive, memory, and effector cell subsets for co-expression of activation (HLA-DR and CD38) and exhaustion/senescence (CD57and PD1) markers. CD19+ B-cell subsets were analyzed for the markers CD21 and CD27. ASC (plasmablasts) were identified as CD19+ cells expressing CD38 and CD27. We used CD16, CD56, and CD57 to identify NK-cell subsets. γδ T cells were identified using an anti-TCR γδ antibody. HLA-DR, CD33, CD45RA, CD123, CD141, and CD1c were used to identify dendritic cell (DC) subsets, as previously described (See et al., 2017). Extracellular labelling was performed for all antibodies except for Ki 67 for which an intracellular labelling was performed with the BD cytofix/cytoperm kit (BD Biosciences).

RNA sequencing

Total RNA was purified from whole blood using the Tempus™ Spin RNA Isolation Kit (ThermoFisher Scientific). RNA was quantified using the Quant-iT RiboGreen RNA Assay Kit (Thermo Fisher Scientific) and quality control performed on a Bioanalyzer (Agilent). Globin mRNA was depleted using Globinclear Kit (Invitrogen) prior to mRNA library preparation with the TruSeq® Stranded mRNA Kit, according to the Illumina protocol. Libraries were sequenced on an Illumina HiSeq 2500 V4 system. Sequencing quality control was performed using Sequence Analysis Viewer (SAV). FastQ files were generated on the Illumina BaseSpace Sequence Hub. Transcript reads were aligned to the hg18 human reference genome using Salmon v0.8.2 (Patro et al., 2017) and quantified relative to annotation model "hsapiens_gene_ensembl" recovered from the R package biomaRt v2.42.1 (Durinck et al., 2009). Quality control of the alignment was performed via MultiQC v1.4 (Patro et al., 2017). Finally, counts were normalized as counts per million.

Quantification and statistical analysis

Subgroups of COVID-19 patients were identified from unsupervised hierarchical clustering of log2-counts-per-million RNA-seq transcriptomics from whole-blood using the Euclidean distance and Ward's method. Differential expression analysis was carried out using dearseq (Gauthier et al., 2019) to contribute to the analysis of genes of which the abundance differed across the three COVID-19 patient subgroups and healthy subjects. Once the groups were defined by hierarchical clustering, the analysis of the genes contributing to each group was performed by selecting genes with an absolute fold-change ≥ 1.5 in the comparison of interest for which the difference in expression between HDs and COVID-19 patients was significant ($P \leq 0.05$) (to avoid so called "double dipping" [https://arxiv.org/abs/2012.02936]). Pathway analyses of the genes involved in each comparison was performed using Ingenuity Pathway Analysis (IPA ®, Qiagen, Redwood City, California, Version 57662101, 2020). For canonical pathway analysis, a Z-score ≥ 2 was defined as the threshold for significant activation, whereas a Z-score ≤ –2 was defined as the threshold for significant inhibition.

The integrative analysis of the three types of biological data (RNA-Seq, cell phenotypes, serum analytes) was performed using MOFA+ (Argelaguet et al., 2019) (, a sparse Factor Analysis method. It provides latent variables which are linear combination of the most influential factors for explaining inter-patient variability across the three biological measurement modalities. The first component is presented and called integrative score here. The analyses of factors associated with CD177 protein concentration were performed using non parametric Wilcoxon test or Spearman correlation coefficient when appropriate. To look at the independent association of CD177 with ICU, a logistic regression for the prediction of hospitalization in ICU adjusted for age, sex, chronic cardiac disease, chronic pulmonary disease, diabetes was fitted. The analysis of repeated measurements of CD177 over time was done by using a linear mixed effect model adjusted for time from hospitalization and an interaction with survival outcome (death or recovery). The model included a random intercept and a random slope with an unstructured matrix for variance parameters. Predictions of

marginal trajectories were performed. All analyses, if not stated otherwise, were performed using R software version 3.6.3 (R Core Team (2020)). R: A language and environment for statistical computing. R Foundation for Statistical Computing, Vienna, Austria. URL: https://www.R-project.org/

Additional Ressources

A subgroup of COVID19 patients of the prospective French COVID cohort was enrolled in this study. French COVID cohort was registered at: https://clinicaltrials.gov/ct2/show/NCT04262921**Table 1. Patient characteristics of the French COVID cohort (n=61)**

	Number of patients	
Demographic characteristics		
Age - Median (IQR) - years	61	60 (50 - 69)
Male sex – No./total No. (%)	61	49/61 (80)
ICU or transfer to ICU or death – No./total No. (%)	61	53/61 (87)
Outcome – No./total No. (%)	61	
Death		21/61 (34)
Discharge alive		40/61 (66)
Median interval from first symptoms on admission (IQR)-days	61	11 (7 - 14)
Comorbidities – No./total No. (%)		
Any	61	14/61 (23)
Chronic cardiac disease	61	9/61 (15)
Hypertension	61	22/61 (36)
Chronic pulmonary disease	61	5/61 (8)

Asthma	61	4/61 (7)
Chronic kidney disease	61	6/61 (10)
Chronic neurological disorder	61	2/61 (3)
Obesity	60	23/60 (38)
Diabetes	61	12/61 (20)
Smoking History – No./total No. (%)		
Smoking	61	5/61 (8)
Laboratory findings on admission - Median (IQR)		
Hemoglobin - g/dL	57	13 (11 - 14)
WBC count - $x10^9$/L	57	6 (5 - 9)
Platelet count - $x10^9$/L	57	189 (143 - 270)
C-reactive protein (CRP) - mg/L	57	120 (66 - 195)
Blood Urea Nitrogen (urea) - mmol/L	57	7 (5 - 12)
Symptoms on admission - No./total No. (%)		
Fever	59	51/59 (86)
Cough	57	40/57 (70)
Sore throat	56	4/56 (7)
Wheezing	54	6/54 (11)
Myalgia	56	21/56 (38)
Arthralgia	55	9/55 (16)
Fatigue	57	27/57 (47)
Dyspnea	57	46/57 (81)
Headache	57	11/57 (19)
Altered consciousness	56	3/56 (5)
Abdominal pain	53	8/53 (15)
Vomiting / nausea	56	10/56 (18)

Diarrhea	56	11/56 (20)
Clinical characteristics on admission - Median (IQR)		
SOFA score (ICU patients)	34	6 (4 - 8)
SAPS2 (ICU patients)	36	32 (27 - 53)
Heart rate - beats per minute	61	87 (76 - 104)
Respiratory rate - breaths per minute	55	24 (20 - 32)
Systolic blood pressure - mmHg	60	130 (109 - 145)
Diastolic blood pressure - mmHg	60	77 (70 - 87)
Oxygen saturation - percent	61	96 (91 - 98)
Oxygen saturation on – No./total No. (%)	56	
Room air		17/56 (30)
Oxygen therapy		39/56 (70)
Treatments – No./total No. (%)		
Antiviral	60	40/60 (66)
Antibiotic	60	46/60 (77)
Corticosteroids	60	33/60 (55)
Antifungal	60	9/60 (15)
Hydroxychloroquine	59	8/59 (14)

637

638

639 **Table 2. Characteristics of patients involved in the CD177 analysis**

	Number of patients	French cohort (n = 115)	Swiss cohort (n = 88)
Demographic characteristics			
Age - Median (IQR) - years	200	62 (54-72)	63 (57-74)
Male sex - No./total No. (%)	201	82/113 (73)	56/88 (64)
ICU or transfer to ICU or death - No. /total No. (%)	200	61/112 (54)	40/88 (45)
Outcome - No. /total No. (%)	173		
Death		32/107 (30)	8/66 (12)
Discharge alive		75/107 (70)	58/66 (88)
Median interval from first symptoms on admission (IQT)	192	13 (9-18)	12 (9-17)
Comorbidities - No./total No. (%)			
Chronic cardiac disease	197	22/109 (20)	25/88 (28)
Chronic pulmonary disease	197	14/109 (13)	9/88 (10)
Diabetes	197	23/109 (21)	26/88 (30)
Laboratory findings on admission - Median (IQR)			
C-reactive protein (CRP) - mg/L	34	122 (62-196)	
Lactate dehydrogenase (LDH) UI/L	31	466 (337-533)	
Clinical characteristics on admission - Median (IQR)			
Score SOFA	41	4 (2-7)	
Score SAPS2	40	32 (27-49)	

640

641 **References**

642 Ali, S., Mann-Nüttel, R., Schulze, A., Richter, L., Alferink, J., and Scheu, S. (2019). Sources
643 of Type I Interferons in Infectious Immunity: Plasmacytoid Dendritic Cells Not Always in the
644 Driver's Seat. Frontiers in Immunology *10*.

645 Argelaguet, R., Clark, S.J., Mohammed, H., Stapel, L.C., Krueger, C., Kapourani, C.A., Imaz-
646 Rosshandler, I., Lohoff, T., Xiang, Y.L., Hanna, C.W.*, et al.* (2019). Multi-omics profiling of
647 mouse gastrulation at single-cell resolution. Nature *576*, 487-+.

648 Arunachalam, P.S., Wimmers, F., Mok, C.K.P., Perera, R., Scott, M., Hagan, T., Sigal, N.,
649 Feng, Y., Bristow, L., Tak-Yin Tsang, O.*, et al.* (2020). Systems biological assessment of
650 immunity to mild versus severe COVID-19 infection in humans. Science.

651 Aschenbrenner, A.C., Mouktaroudi, M., Krämer, B., Oestreich, M., Antonakos, N., Nuesch-
652 Germano, M., Gkizeli, K., Bonaguro, L., Reusch, N., Baßler, K.*, et al.* (2021). Disease
653 severity-specific neutrophil signatures in blood transcriptomes stratify COVID-19 patients.
654 Genome Medicine *13*.

655 Augustin, A., Kubo, R.T., and Sim, G.K. (1989). Resident pulmonary lymphocytes expressing
656 the gamma/delta T-cell receptor. Nature *340*, 239-241.

657 Barnes, B.J., Adrover, J.M., Baxter-Stoltzfus, A., Borczuk, A., Cools-Lartigue, J., Crawford,
658 J.M., Daßler-Plenker, J., Guerci, P., Huynh, C., Knight, J.S.*, et al.* (2020a). Targeting
659 potential drivers of COVID-19: Neutrophil extracellular traps. Journal of Experimental
660 Medicine *217*.

661 Barnes, C.O., West, A.P., Jr., Huey-Tubman, K.E., Hoffmann, M.A.G., Sharaf, N.G.,
662 Hoffman, P.R., Koranda, N., Gristick, H.B., Gaebler, C., Muecksch, F.*, et al.* (2020b).
663 Structures of Human Antibodies Bound to SARS-CoV-2 Spike Reveal Common Epitopes and
664 Recurrent Features of Antibodies. Cell *182*, 828-842 e816.

665 Bastard, P., Rosen, L.B., Zhang, Q., Michailidis, E., Hoffmann, H.-H., Zhang, Y., Dorgham,
666 K., Philippot, Q., Rosain, J., Béziat, V.*, et al.* (2020). Autoantibodies against type I IFNs in
667 patients with life-threatening COVID-19. Science *370*, eabd4585.

668 Bayat, B., Werth, S., Sachs, U.J.H., Newman, D.K., Newman, P.J., and Santoso, S. (2010).
669 Neutrophil Transmigration Mediated by the Neutrophil-Specific Antigen CD177 Is Influenced
670 by the Endothelial S536N Dimorphism of Platelet Endothelial Cell Adhesion Molecule-1. The
671 Journal of Immunology *184*, 3889-3896.
672 Blanco-Melo, D., Nilsson-Payant, B.E., Liu, W.C., Uhl, S., Hoagland, D., Moller, R., Jordan,
673 T.X., Oishi, K., Panis, M., Sachs, D.*, et al.* (2020). Imbalanced Host Response to SARS-
674 CoV-2 Drives Development of COVID-19. Cell *181*, 1036-1045 e1039.
675 Bouadma, L., Wiedemann, A., Patrier, J., Surenaud, M., Wicky, P.H., Foucat, E., Diehl, J.L.,
676 Hejblum, B.P., Sinnah, F., de Montmollin, E.*, et al.* (2020). Immune Alterations in a Patient
677 with SARS-CoV-2-Related Acute Respiratory Distress Syndrome. J Clin Immunol.
678 Boyd, J.H., Fjell, C.D., Russell, J.A., Sirounis, D., Cirstea, M.S., and Walley, K.R. (2016).
679 Increased Plasma PCSK9 Levels Are Associated with Reduced Endotoxin Clearance and
680 the Development of Acute Organ Failures during Sepsis. J Innate Immun *8*, 211-220.
681 Brandes, M., Klauschen, F., Kuchen, S., and Germain, R.N. (2013). A systems analysis
682 identifies a feedforward inflammatory circuit leading to lethal influenza infection. Cell *154*,
683 197-212.
684 Brouwer, P.J.M., Caniels, T.G., van der Straten, K., Snitselaar, J.L., Aldon, Y., Bangaru, S.,
685 Torres, J.L., Okba, N.M.A., Claireaux, M., Kerster, G.*, et al.* (2020). Potent neutralizing
686 antibodies from COVID-19 patients define multiple targets of vulnerability. Science *369*, 643-
687 650.
688 Buechler, C., Eisinger, K., and Krautbauer, S. (2013). Diagnostic and prognostic potential of
689 the macrophage specific receptor CD163 in inflammatory diseases. Inflamm Allergy Drug
690 Targets *12*, 391-402.
691 Cai, Y.Q., Lv, Y., Mo, Z.C., Lei, J., Zhu, J.L., and Zhong, Q.Q. (2020). Multiple
692 pathophysiological roles of midkine in human disease. Cytokine *135*, 155242.
693 Chen, G., Wu, D., Guo, W., Cao, Y., Huang, D., Wang, H., Wang, T., Zhang, X., Chen, H.,
694 Yu, H.*, et al.* (2020a). Clinical and immunological features of severe and moderate
695 coronavirus disease 2019. J Clin Invest.

Chen, N., Zhou, M., Dong, X., Qu, J., Gong, F., Han, Y., Qiu, Y., Wang, J., Liu, Y., Wei, Y.*, et al.* (2020b). Epidemiological and clinical characteristics of 99 cases of 2019 novel coronavirus pneumonia in Wuhan, China: a descriptive study. Lancet *395*, 507-513.

Cheng, M., and Hu, S. (2017). Lung-resident gammadelta T cells and their roles in lung diseases. Immunology *151*, 375-384.

Coronaviridae Study Group of the International Committee on Taxonomy of, V. (2020). The species Severe acute respiratory syndrome-related coronavirus: classifying 2019-nCoV and naming it SARS-CoV-2. Nat Microbiol *5*, 536-544.

Darbousset, R., Thomas, G.M., Mezouar, S., Frère, C., Bonier, R., Mackman, N., Renné, T., Dignat-George, F., Dubois, C., and Panicot-Dubois, L. (2012). Tissue factor–positive neutrophils bind to injured endothelial wall and initiate thrombus formation. Blood *120*, 2133-2143.

De Biasi, S., Meschiari, M., Gibellini, L., Bellinazzi, C., Borella, R., Fidanza, L., Gozzi, L., Iannone, A., Lo Tartaro, D., Mattioli, M.*, et al.* (2020). Marked T cell activation, senescence, exhaustion and skewing towards TH17 in patients with COVID-19 pneumonia. Nat Commun *11*, 3434.

Demaret, J., Venet, F., Plassais, J., Cazalis, M.-A., Vallin, H., Friggeri, A., Lepape, A., Rimmelé, T., Textoris, J., and Monneret, G. (2016). Identification of CD177 as the most dysregulated parameter in a microarray study of purified neutrophils from septic shock patients. Immunology Letters *178*, 122-130.

Durinck, S., Spellman, P.T., Birney, E., and Huber, W. (2009). Mapping identifiers for the integration of genomic datasets with the R/Bioconductor package biomaRt. Nature Protocols *4*, 1184-1191.

Dwivedi, D.J., Grin, P.M., Khan, M., Prat, A., Zhou, J., Fox-Robichaud, A.E., Seidah, N.G., and Liaw, P.C. (2016). Differential Expression of PCSK9 Modulates Infection, Inflammation, and Coagulation in a Murine Model of Sepsis. Shock *46*, 672-680.

722 Fu, J., Kong, J., Wang, W., Wu, M., Yao, L., Wang, Z., Jin, J., Wu, D., and Yu, X. (2020). The
723 clinical implication of dynamic neutrophil to lymphocyte ratio and D-dimer in COVID-19: A
724 retrospective study in Suzhou China. Thrombosis Research *192*, 3-8.
725 Gan, E.S., Tan, H.C., Duyen, H.L.T., Trieu, H.T., Wills, B., Ooi, E.E., Seidah, N.G., and
726 Yacoub, S. (2020). Dengue virus induces PCSK9 expression to alter antiviral responses and
727 disease outcomes. J Clin Invest.
728 Gauthier, M., Agniel, D., Thiébaut, R., and Hejblum, B.P. (2019). dearseq: a variance
729 component score test for RNA-Seq differential analysis that effectively controls the false
730 discovery rate.
731 Giamarellos-Bourboulis, E.J., Netea, M.G., Rovina, N., Akinosoglou, K., Antoniadou, A.,
732 Antonakos, N., Damoraki, G., Gkavogianni, T., Adami, M.E., Katsaounou, P.*, et al.* (2020).
733 Complex Immune Dysregulation in COVID-19 Patients with Severe Respiratory Failure. Cell
734 Host Microbe *27*, 992-1000 e1003.
735 Hadjadj, J., Yatim, N., Barnabei, L., Corneau, A., Boussier, J., Smith, N., Pere, H., Charbit,
736 B., Bondet, V., Chenevier-Gobeaux, C.*, et al.* (2020). Impaired type I interferon activity and
737 inflammatory responses in severe COVID-19 patients. Science *369*, 718-724.
738 Huang, C., Wang, Y., Li, X., Ren, L., Zhao, J., Hu, Y., Zhang, L., Fan, G., Xu, J., Gu, X.*, et al.*
739 (2020). Clinical features of patients infected with 2019 novel coronavirus in Wuhan, China.
740 Lancet *395*, 497-506.
741 Huang, W.D., Lin, Y.T., Tsai, Z.Y., Chang, L.S., Liu, S.F., Lin, Y.J., and Kuo, H.C. (2019).
742 Association between maternal age and outcomes in Kawasaki disease patients. Pediatr
743 Rheumatol *17*.
744 Jing, Y., Ding, M., Fu, J., Xiao, Y., Chen, X., and Zhang, Q. (2020). Neutrophil extracellular
745 trap from Kawasaki disease alter the biologic responses of PBMC. Biosci Rep.
746 Juss, J.K., House, D., Amour, A., Begg, M., Herre, J., Storisteanu, D.M.L., Hoenderdos, K.,
747 Bradley, G., Lennon, M., Summers, C.*, et al.* (2016). Acute Respiratory Distress Syndrome
748 Neutrophils Have a Distinct Phenotype and Are Resistant to Phosphoinositide 3-Kinase
749 Inhibition. Am J Resp Crit Care *194*, 961-973.

Kaur, S., Sassano, A., Majchrzak-Kita, B., Baker, D.P., Su, B., Fish, E.N., and Platanias, L.C. (2012). Regulatory effects of mTORC2 complexes in type I IFN signaling and in the generation of IFN responses. Proceedings of the National Academy of Sciences *109*, 7723-7728.

Kim, S.H., Han, S.Y., Azam, T., Yoon, D.Y., and Dinarello, C.A. (2005). Interleukin-32: a cytokine and inducer of TNFalpha. Immunity *22*, 131-142.

Ko, T.M., Chang, J.S., Chen, S.P., Liu, Y.M., Chang, C.J., Tsai, F.J., Lee, Y.C., Chen, C.H., Chen, Y.T., and Wu, J.Y. (2019). Genome-wide transcriptome analysis to further understand neutrophil activation and lncRNA transcript profiles in Kawasaki disease. Sci Rep *9*, 328.

Kuri-Cervantes, L., Pampena, M.B., Meng, W., Rosenfeld, A.M., Ittner, C.A.G., Weisman, A.R., Agyekum, R., Mathew, D., Baxter, A.E., Vella, L.*, et al.* (2020). Immunologic perturbations in severe COVID-19/SARS-CoV-2 infection. bioRxiv.

Laing, A.G., Lorenc, A., Del Molino Del Barrio, I., Das, A., Fish, M., Monin, L., Munoz-Ruiz, M., McKenzie, D.R., Hayday, T.S., Francos-Quijorna, I.*, et al.* (2020). A dynamic COVID-19 immune signature includes associations with poor prognosis. Nat Med.

Le Gall, J.R. (1993). A new Simplified Acute Physiology Score (SAPS II) based on a European/North American multicenter study. JAMA: The Journal of the American Medical Association *270*, 2957-2963.

Levin, D., and London, I.M. (1978). Regulation of protein synthesis: activation by double-stranded RNA of a protein kinase that phosphorylates eukaryotic initiation factor 2. Proc Natl Acad Sci U S A *75*, 1121-1125.

Lucas, C., Wong, P., Klein, J., Castro, T.B.R., Silva, J., Sundaram, M., Ellingson, M.K., Mao, T., Oh, J.E., Israelow, B.*, et al.* (2020). Longitudinal analyses reveal immunological misfiring in severe COVID-19. Nature *584*, 463-469.

Mathew, D., Giles, J.R., Baxter, A.E., Oldridge, D.A., Greenplate, A.R., Wu, J.E., Alanio, C., Kuri-Cervantes, L., Pampena, M.B., D'Andrea, K.*, et al.* (2020). Deep immune profiling of COVID-19 patients reveals distinct immunotypes with therapeutic implications. Science *369*, eabc8511.

778 Mehta, P., McAuley, D.F., Brown, M., Sanchez, E., Tattersall, R.S., and Manson, J.J. (2020).
779 COVID-19: consider cytokine storm syndromes and immunosuppression. The Lancet *395*,
780 1033-1034.
781 Migliorini, P., Italiani, P., Pratesi, F., Puxeddu, I., and Boraschi, D. (2020). The IL-1 family
782 cytokines and receptors in autoimmune diseases. Autoimmun Rev *19*, 102617.
783 Narasaraju, T., Yang, E., Samy, R.P., Ng, H.H., Poh, W.P., Liew, A.A., Phoon, M.C., van
784 Rooijen, N., and Chow, V.T. (2011). Excessive neutrophils and neutrophil extracellular traps
785 contribute to acute lung injury of influenza pneumonitis. Am J Pathol *179*, 199-210.
786 Ong, E.Z., Chan, Y.F.Z., Leong, W.Y., Lee, N.M.Y., Kalimuddin, S., Haja Mohideen, S.M.,
787 Chan, K.S., Tan, A.T., Bertoletti, A., Ooi, E.E.*, et al.* (2020). A Dynamic Immune Response
788 Shapes COVID-19 Progression. Cell Host Microbe *27*, 879-882 e872.
789 Pakos-Zebrucka, K., Koryga, I., Mnich, K., Ljujic, M., Samali, A., and Gorman, A.M. (2016).
790 The integrated stress response. EMBO Rep *17*, 1374-1395.
791 Patro, R., Duggal, G., Love, M.I., Irizarry, R.A., and Kingsford, C. (2017). Salmon provides
792 fast and bias-aware quantification of transcript expression. Nature Methods *14*, 417-419.
793 Phelan, A.L., Katz, R., and Gostin, L.O. (2020). The Novel Coronavirus Originating in
794 Wuhan, China: Challenges for Global Health Governance. JAMA.
795 Ponti, G., Maccaferri, M., Ruini, C., Tomasi, A., and Ozben, T. (2020). Biomarkers
796 associated with COVID-19 disease progression. Critical Reviews in Clinical Laboratory
797 Sciences *57*, 389-399.
798 Prescott, H.C., and Rice, T.W. (2020). Corticosteroids in COVID-19 ARDS. Jama *324*, 1292.
799 Qin, C., Zhou, L., Hu, Z., Zhang, S., Yang, S., Tao, Y., Xie, C., Ma, K., Shang, K., Wang, W.*,*
800 *et al.* (2020). Dysregulation of immune response in patients with COVID-19 in Wuhan, China.
801 Clin Infect Dis.
802 Rabouw, H.H., Langereis, M.A., Knaap, R.C., Dalebout, T.J., Canton, J., Sola, I., Enjuanes,
803 L., Bredenbeek, P.J., Kikkert, M., de Groot, R.J.*, et al.* (2016). Middle East Respiratory
804 Coronavirus Accessory Protein 4a Inhibits PKR-Mediated Antiviral Stress Responses. PLoS
805 Pathog *12*, e1005982.

Rabouw, H.H., Visser, L.J., Passchier, T.C., Langereis, M.A., Liu, F., Giansanti, P., van Vliet, A.L.W., Dekker, J.G., van der Grein, S.G., Saucedo, J.G., *et al.* (2020). Inhibition of the integrated stress response by viral proteins that block p-eIF2-eIF2B association. Nat Microbiol.

Roth, J., Vogl, T., Sorg, C., and Sunderkötter, C. (2003). Phagocyte-specific S100 proteins: a novel group of proinflammatory molecules. Trends in Immunology *24*, 155-158.

Schulte-Schrepping, J., Reusch, N., Paclik, D., Baßler, K., Schlickeiser, S., Zhang, B., Krämer, B., Krammer, T., Brumhard, S., Bonaguro, L., *et al.* (2020). Severe COVID-19 Is Marked by a Dysregulated Myeloid Cell Compartment. Cell *182*, 1419-1440.e1423.

See, P., Dutertre, C.A., Chen, J., Gunther, P., McGovern, N., Irac, S.E., Gunawan, M., Beyer, M., Handler, K., Duan, K., *et al.* (2017). Mapping the human DC lineage through the integration of high-dimensional techniques. Science *356*.

Shen-Orr, S.S., Tibshirani, R., Khatri, P., Bodian, D.L., Staedtler, F., Perry, N.M., Hastie, T., Sarwal, M.M., Davis, M.M., and Butte, A.J. (2010). Cell type–specific gene expression differences in complex tissues. Nature Methods *7*, 287-289.

Silvin, A., Chapuis, N., Dunsmore, G., Goubet, A.G., Dubuisson, A., Derosa, L., Almire, C., Henon, C., Kosmider, O., Droin, N., *et al.* (2020). Elevated Calprotectin and Abnormal Myeloid Cell Subsets Discriminate Severe from Mild COVID-19. Cell.

Sterne, J.A.C., Murthy, S., Diaz, J.V., Slutsky, A.S., Villar, J., Angus, D.C., Annane, D., Azevedo, L.C.P., Berwanger, O., Cavalcanti, A.B., *et al.* (2020). Association Between Administration of Systemic Corticosteroids and Mortality Among Critically Ill Patients With COVID-19. Jama *324*, 1330.

Tang, B.M., Shojaei, M., Teoh, S., Meyers, A., Ho, J., Ball, T.B., Keynan, Y., Pisipati, A., Kumar, A., Eisen, D.P., *et al.* (2019). Neutrophils-related host factors associated with severe disease and fatality in patients with influenza infection. Nat Commun *10*, 3422.

Theilgaard-Monch, K. (2006). Haptoglobin is synthesized during granulocyte differentiation, stored in specific granules, and released by neutrophils in response to activation. Blood *108*, 353-361.

834 Toubiana, J., Poirault, C., Corsia, A., Bajolle, F., Fourgeaud, J., Angoulvant, F., Debray, A.,
835 Basmaci, R., Salvador, E., Biscardi, S.*, et al.* (2020). Kawasaki-like multisystem inflammatory
836 syndrome in children during the covid-19 pandemic in Paris, France: prospective
837 observational study. BMJ *369*, m2094.
838 Vincent, J.-L., de Mendonca, A., Cantraine, F., Moreno, R., Takala, J., Suter, P.M., Sprung,
839 C.L., Colardyn, F., and Blecher, S. (1998). Use of the SOFA score to assess the incidence of
840 organ dysfunction/failure in intensive care units. Critical Care Medicine *26*, 1793-1800.
841 Viner, R.M., and Whittaker, E. (2020). Kawasaki-like disease: emerging complication during
842 the COVID-19 pandemic. Lancet *395*, 1741-1743.
843 Wilk, A.J., Rustagi, A., Zhao, N.Q., Roque, J., Martinez-Colon, G.J., McKechnie, J.L., Ivison,
844 G.T., Ranganath, T., Vergara, R., Hollis, T.*, et al.* (2020). A single-cell atlas of the peripheral
845 immune response in patients with severe COVID-19. Nat Med *26*, 1070-1076.
846 Wu, Z.Y., and McGoogan, J.M. (2020). Characteristics of and Important Lessons From the
847 Coronavirus Disease 2019 (COVID-19) Outbreak in China Summary of a Report of 72 314
848 Cases From the Chinese Center for Disease Control and Prevention. Jama-J Am Med Assoc
849 *323*, 1239-1242.
850 Xu, B., Fan, C.Y., Wang, A.L., Zou, Y.L., Yu, Y.H., He, C., Xia, W.G., Zhang, J.X., and Miao,
851 Q. (2020). Suppressed T cell-mediated immunity in patients with COVID-19: A clinical
852 retrospective study in Wuhan, China. J Infect *81*, e51-e60.
853 Yazdanpanah, Y. (2020). Impact on disease mortality of clinical, biological, and virological
854 characteristics at hospital admission and overtime in COVID-19 patients. Journal of Medical
855 Virology.
856 Zaas, A.K., Chen, M., Varkey, J., Veldman, T., Hero, A.O., Lucas, J., Huang, Y., Turner, R.,
857 Gilbert, A., Lambkin-Williams, R.*, et al.* (2009). Gene Expression Signatures Diagnose
858 Influenza and Other Symptomatic Respiratory Viral Infections in Humans. Cell Host &
859 Microbe *6*, 207-217.

Zhi, Y., Gao, P., Xin, X., Li, W., Ji, L., Zhang, L., Zhang, X., and Zhang, J. (2017). Clinical significance of sCD163 and its possible role in asthma (Review). Mol Med Rep *15*, 2931-2939.

Zhou, Z., Ren, L., Zhang, L., Zhong, J., Xiao, Y., Jia, Z., Guo, L., Yang, J., Wang, C., Jiang, S.*, et al.* (2020). Heightened Innate Immune Responses in the Respiratory Tract of COVID-19 Patients. Cell Host Microbe *27*, 883-890 e882.

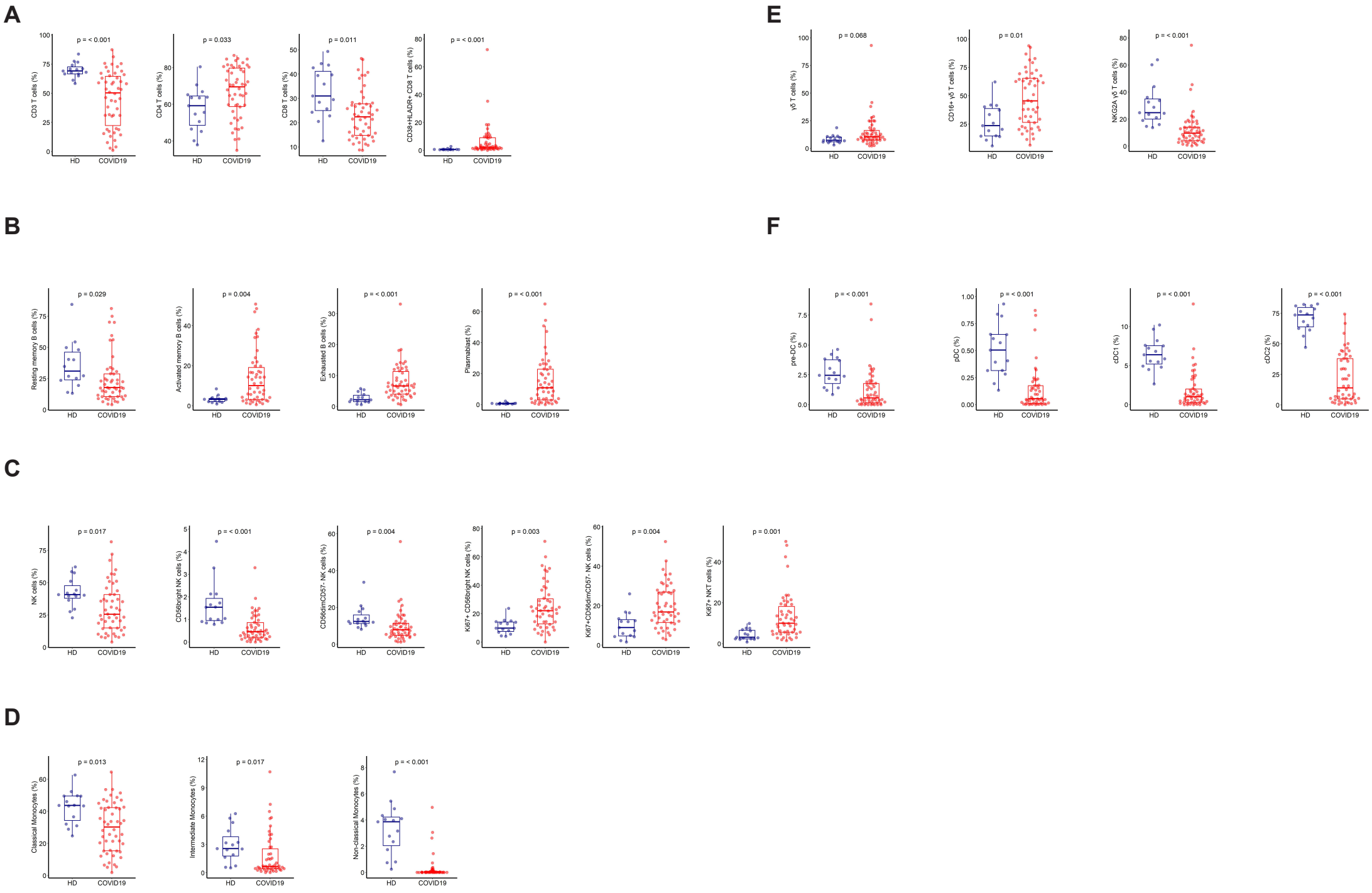
A
CD3 T cells (%)
p = < 0.001
CD4 T cells (%)
p = 0.033
CD8 T cells (%)
p = 0.011
CD38+HLADR+ CD8 T cells (%)
p = < 0.001
B
Resting memory B cells (%)
p = 0.029
Activated memory B cells (%)
p = 0.004
Exhausted B cells (%)
p = < 0.001
Plasmablast (%)
p = < 0.001
C
NK cells (%)
p = 0.017
CD56bright NK cells (%)
p = < 0.001
CD56dimCD57- NK cells (%)
p = 0.004
Ki67+ CD56bright NK cells (%)
p = 0.003
Ki67+CD56dimCD57- NK cells (%)
p = 0.004
Ki67+ NKT cells (%)
p = 0.001
D
Classical Monocytes (%)
p = 0.013
Intermediate Monocytes (%)
p = 0.017
Non-classical Monocytes (%)
p = < 0.001
E
γδ T cells (%)
p = 0.068
CD16+ γδ T cells (%)
p = 0.01
NKG2A γδ T cells (%)
p = < 0.001
F
pre-DC (%)
p = < 0.001
pDC (%)
p = < 0.001
cDC1 (%)
p = < 0.001
cDC2 (%)
p = < 0.001
HD
COVID19

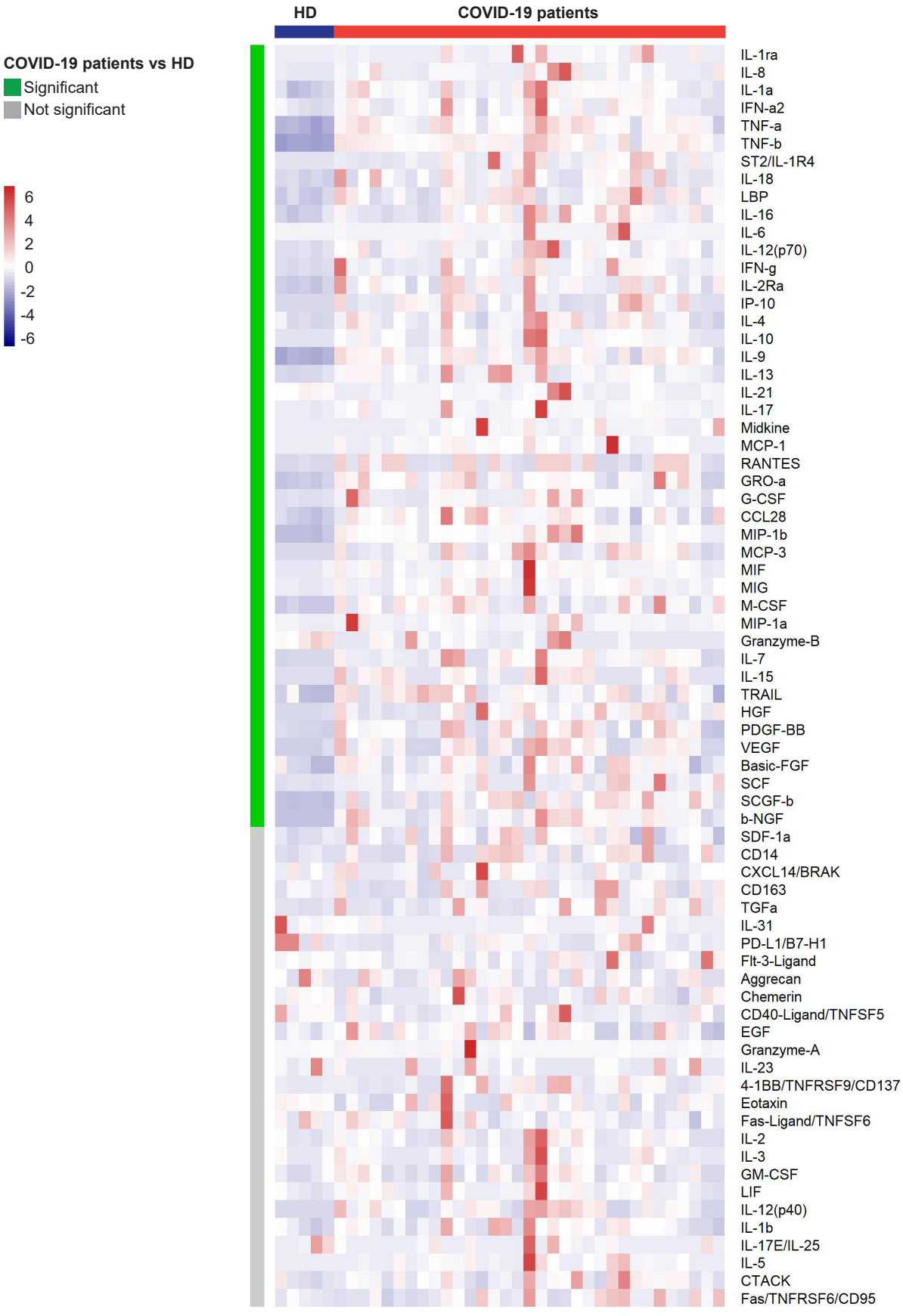
HD
COVID-19 patients
COVID-19 patients vs HD
Significant
Not significant
6
4
2
0
-2
-4
-6
IL-1ra
IL-8
IL-1a
IFN-a2
TNF-a
TNF-b
ST2/IL-1R4
IL-18
LBP
IL-16
IL-6
IL-12(p70)
IFN-g
IL-2Ra
IP-10
IL-4
IL-10
IL-9
IL-13
IL-21
IL-17
Midkine
MCP-1
RANTES
GRO-a
G-CSF
CCL28
MIP-1b
MCP-3
MIF
MIG
M-CSF
MIP-1a
Granzyme-B
IL-7
IL-15
TRAIL
HGF
PDGF-BB
VEGF
Basic-FGF
SCF
SCGF-b
b-NGF
SDF-1a
CD14
CXCL14/BRAK
CD163
TGFa
IL-31
PD-L1/B7-H1
Flt-3-Ligand
Aggrecan
Chemerin
CD40-Ligand/TNFSF5
EGF
Granzyme-A
IL-23
4-1BB/TNFRSF9/CD137
Eotaxin
Fas-Ligand/TNFSF6
IL-2
IL-3
GM-CSF
LIF
IL-12(p40)
IL-1b
IL-17E/IL-25
IL-5
CTACK
Fas/TNFRSF6/CD95

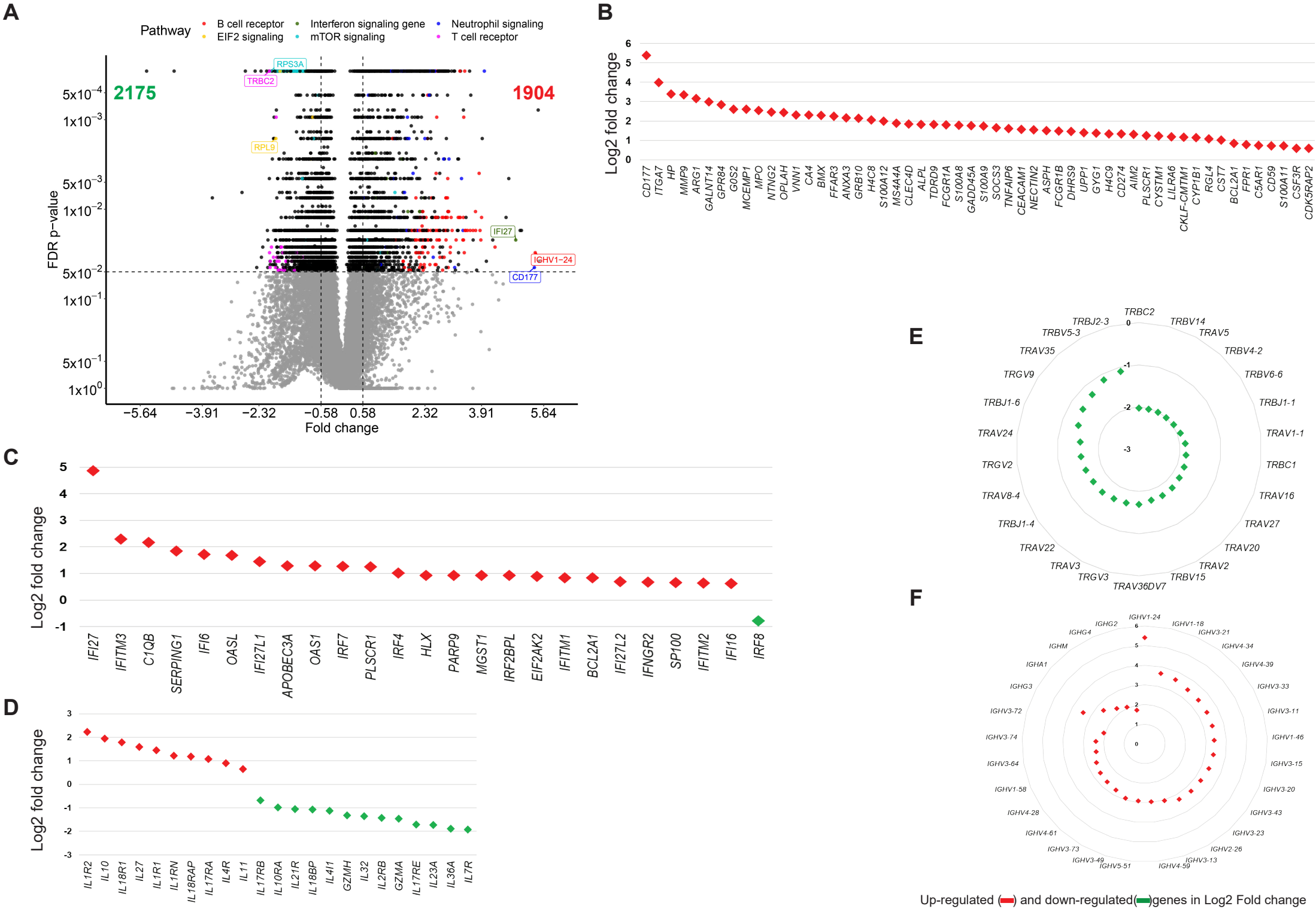
A
Pathway
B cell receptor
EIF2 signaling
Interferon signaling gene
mTOR signaling
Neutrophil signaling
T cell receptor
2175
1904
RPS3A
TRBC2
RPL9
IFI27
IGHV1−24
CD177
FDR p−value
Fold change
B
Log2 fold change
CD177 ITGA7 HP MMP9 ARG1 GALNT14 GPR84 G0S2 MCEMP1 MPO NTNG2 OPLAH VNN1 CA4 BMX FFAR3 ANXA3 GRB10 H4C8 S100A12 MS4A4A CLEC4D ALPL TDRD9 FCGR1A S100A8 GADD45A S100A9 SOCS3 TNFAIP6 CEACAM1 NECTIN2 ASPH FCGR1B DHRS9 UPP1 GYG1 H4C9 CD274 AIM2 PLSCR1 CYSTM1 LILRA6 CKLF-CMTM1 CYP1B1 RGL4 CST7 BCL2A1 FPR1 C5AR1 CD59 S100A11 CSF3R CDK5RAP2
C
Log2 fold change
IFI27 IFITM3 C1QB SERPING1 IFI6 OASL IFI27L1 APOBEC3A OAS1 IRF7 PLSCR1 IRF4 HLX PARP9 MGST1 IRF2BPL EIF2AK2 IFITM1 BCL2A1 IFI27L2 IFNGR2 SP100 IFITM2 IFI16 IRF8
D
Log2 fold change
IL1R2 IL10 IL18R1 IL27 IL1R1 IL1RN IL18RAP IL17RA IL4R IL11 IL17RB IL10RA IL21R IL18BP IL411 GZMH IL32 IL2RB GZMA IL17RE IL23A IL36A IL7R
E
TRBC2 TRBV14 TRAV5 TRBV4-2 TRBV6-6 TRBJ1-1 TRAV1-1 TRBC1 TRAV16 TRAV27 TRAV20 TRAV2 TRBV15 TRAV36DV7 TRGV3 TRAV3 TRAV22 TRBJ1-4 TRAV8-4 TRGV2 TRAV24 TRBJ1-6 TRGV9 TRAV35 TRBV5-3 TRBJ2-3
F
IGHV1-24 IGHV1-18 IGHV3-21 IGHV4-34 IGHV4-39 IGHV3-33 IGHV3-11 IGHV1-46 IGHV3-15 IGHV3-20 IGHV3-43 IGHV3-23 IGHV2-26 IGHV3-13 IGHV4-59 IGHV5-51 IGHV3-49 IGHV3-73 IGHV4-61 IGHV4-28 IGHV1-58 IGHV3-64 IGHV3-74 IGHV3-72 IGHG3 IGHA1 IGHM IGHG4 IGHG2
Up-regulated (red) and down-regulated(green)genes in Log2 Fold change

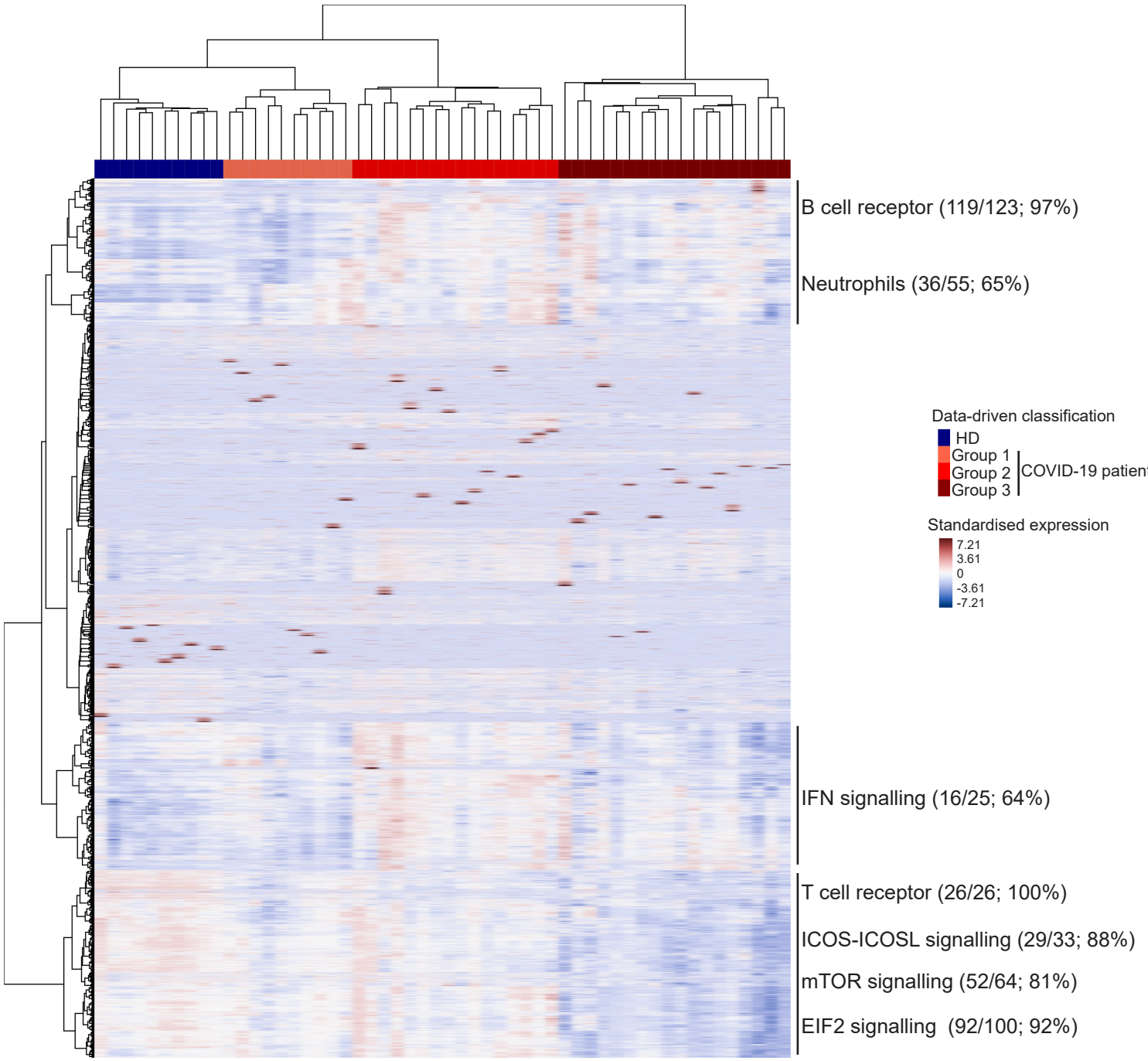
B cell receptor (119/123; 97%)
Neutrophils (36/55; 65%)
IFN signalling (16/25; 64%)
T cell receptor (26/26; 100%)
ICOS-ICOSL signalling (29/33; 88%)
mTOR signalling (52/64; 81%)
EIF2 signalling (92/100; 92%)
Data-driven classification
HD
Group 1
Group 2
Group 3
COVID-19 patients
Standardised expression
7.21
3.61
0
-3.61
-7.21

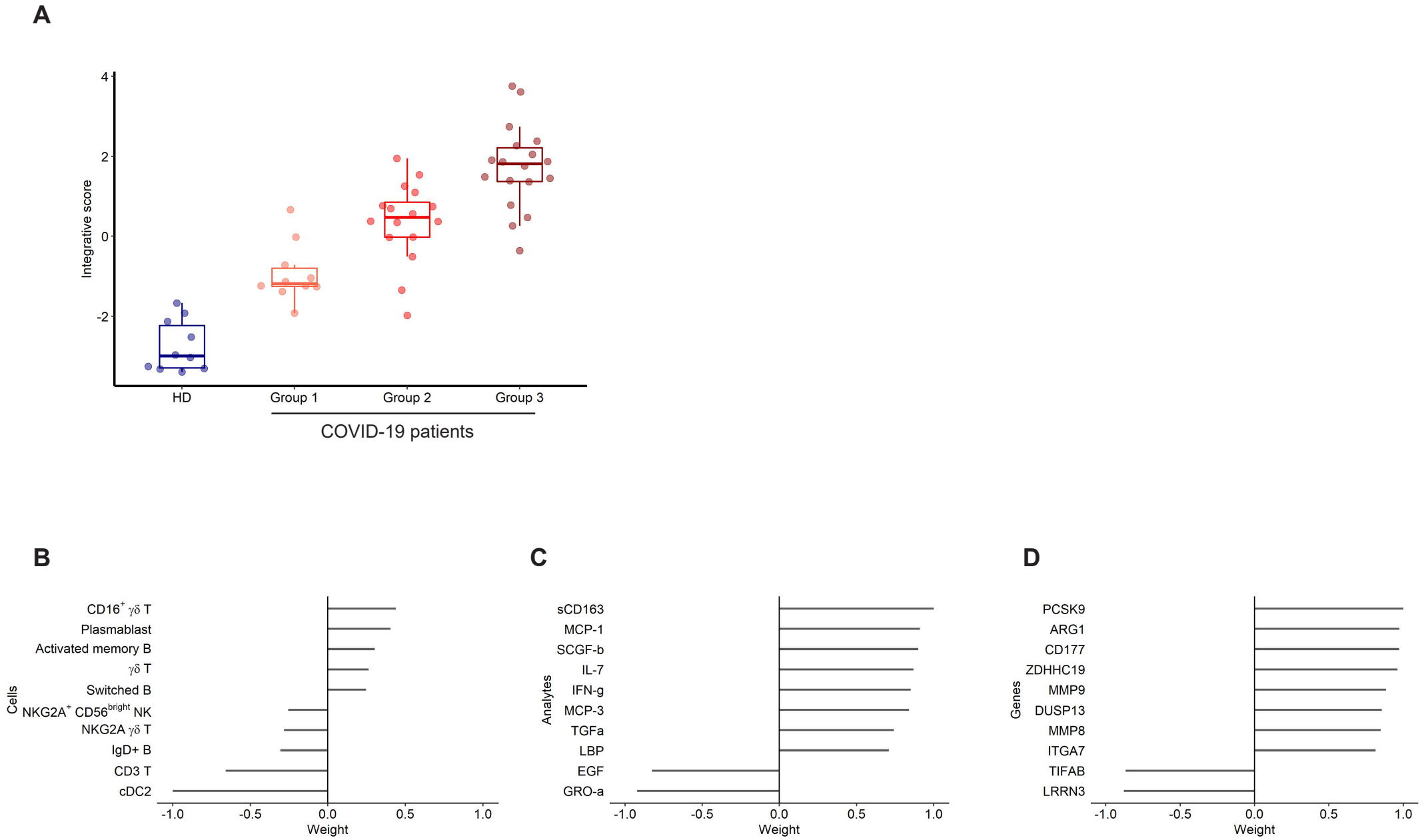
A
Integrative score
4
2
0
-2
HD
Group 1
Group 2
Group 3
COVID-19 patients
B
Cells
CD16+ γδ T
Plasmablast
Activated memory B
γδ T
Switched B
NKG2A+ CD56bright NK
NKG2A γδ T
IgD+ B
CD3 T
cDC2
-1.0
-0.5
0.0
0.5
1.0
Weight
C
Analytes
sCD163
MCP-1
SCGF-b
IL-7
IFN-g
MCP-3
TGFa
LBP
EGF
GRO-a
-1.0
-0.5
0.0
0.5
1.0
Weight
D
Genes
PCSK9
ARG1
CD177
ZDHHC19
MMP9
DUSP13
MMP8
ITGA7
TIFAB
LRRN3
-1.0
-0.5
0.0
0.5
1.0
Weight

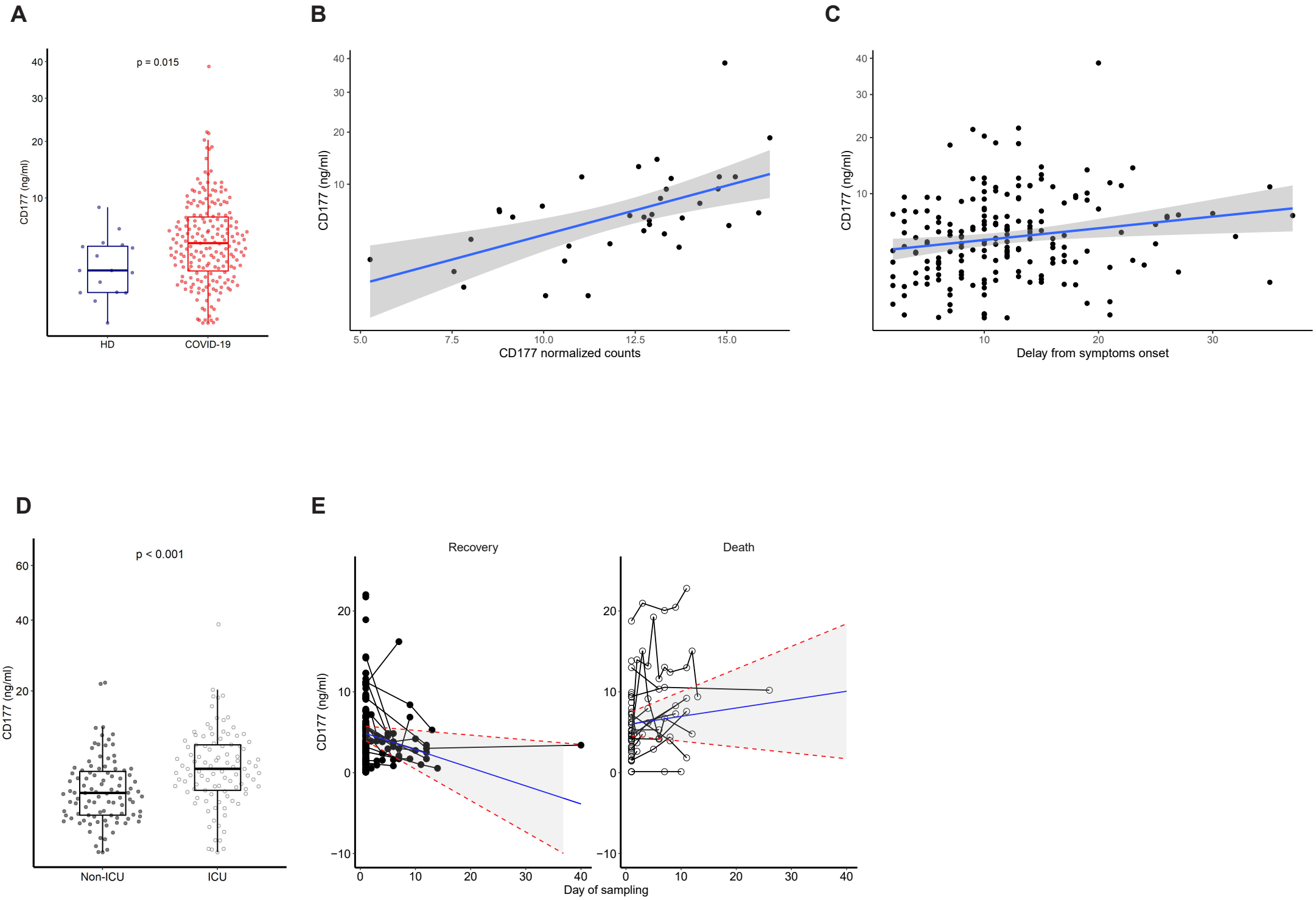
A
p = 0.015
CD177 (ng/ml)
HD
COVID-19
B
CD177 (ng/ml)
CD177 normalized counts
C
CD177 (ng/ml)
Delay from symptoms onset
D
p < 0.001
CD177 (ng/ml)
Non-ICU
ICU
E
Recovery
Death
CD177 (ng/ml)
Day of sampling

Phenotype, cytokine and inflammatory profiles

T Lymphocytes

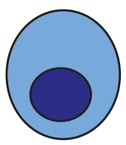

NKG2A on γδ T cells

CD38⁺HLADR⁺ activated CD8 T cells
CD16 expression on γδ T cells

B lymphocytes

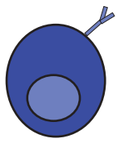

Activated memory B cells
Exhausted B cells
Plasmablasts

NK

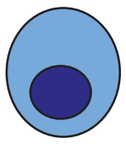

Total NK

NKT

Monocytes

DCs

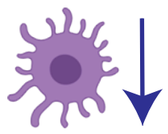

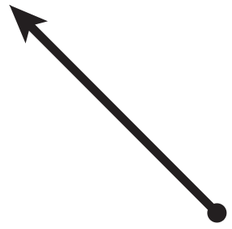

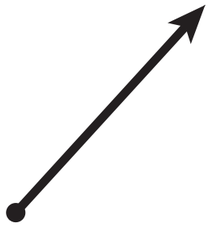

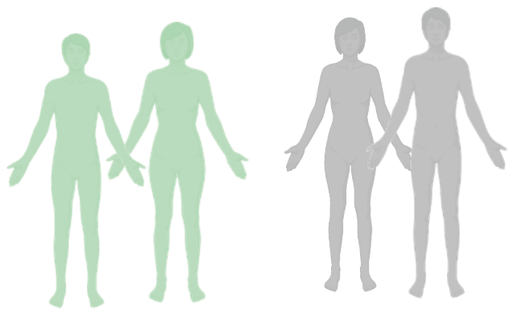

Whole blood gene expression

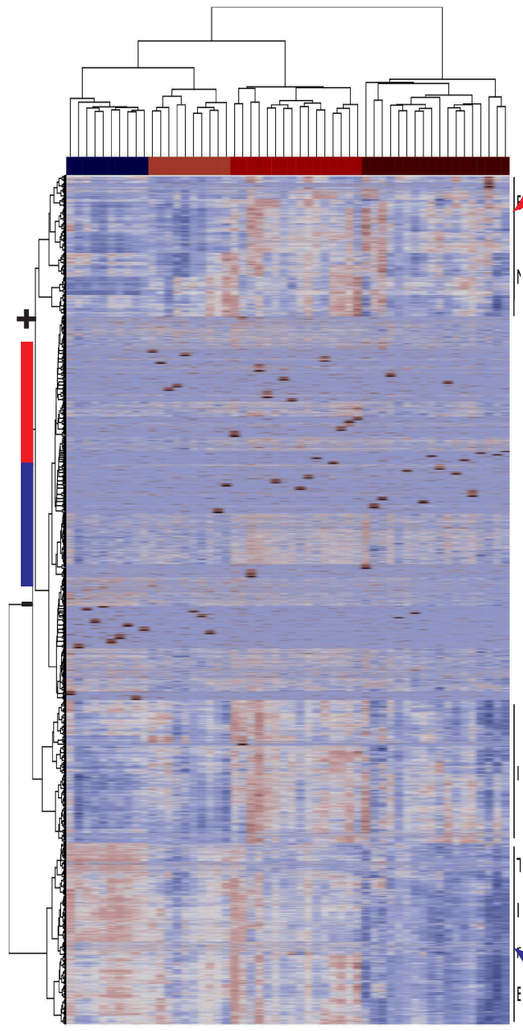

Plasma B cell genes

Neutrophil genes (CD177..)

IFN signaling

T-cell receptor signaling

ICOS-ICOS-L signaling

mTOR signaling

EIF2 signaling

Luminex

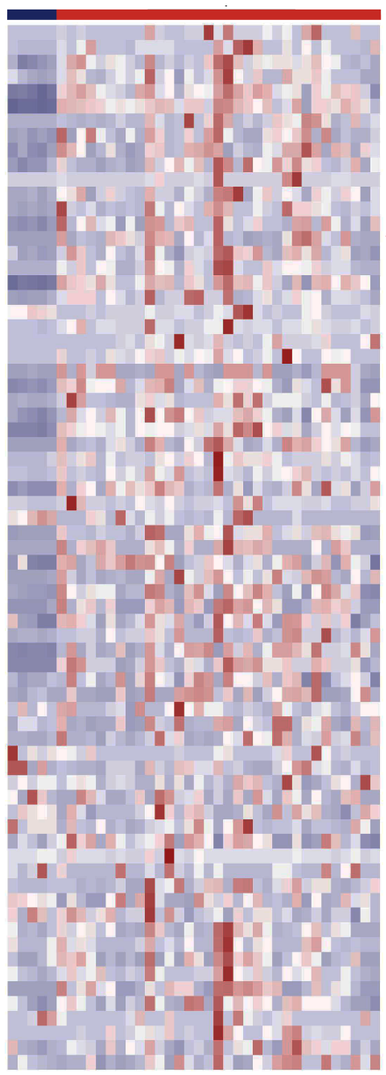

Pro-inflammatory

Neutrophil activation

IL-21

Granzyme B

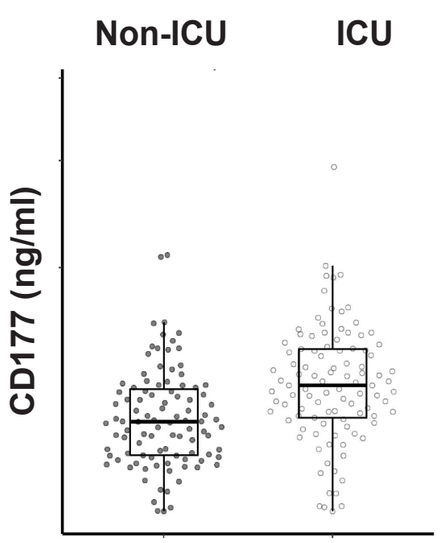

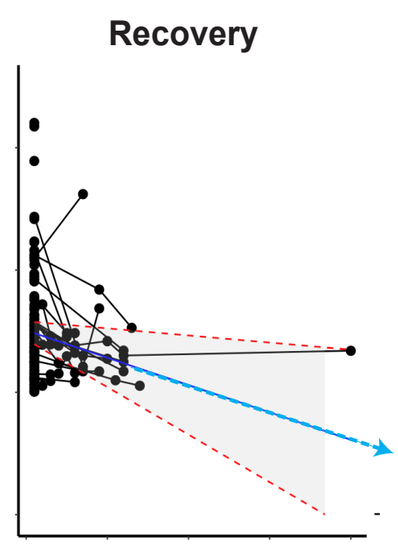

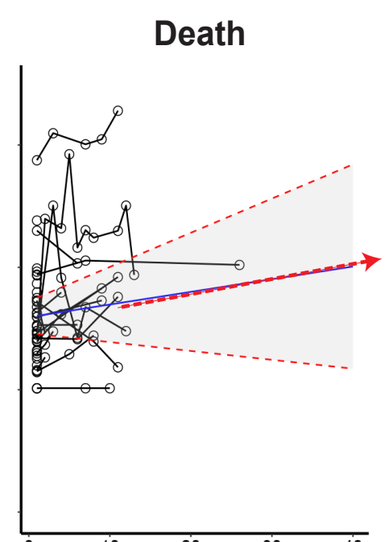

Day of sampling